X-524-73-185
PREPRINT

TRANSMITTER AND RECEIVER ANTENNA GAIN ANALYSIS FOR LASER RADAR AND COMMUNICATION SYSTEMS

BERNARD J. KLEIN
JOHN J. DEGNAN

JUNE 1973

GODDARD SPACE FLIGHT CENTER
GREENBELT, MARYLAND

X-524-73-185

TRANSMITTER AND RECEIVER ANTENNA GAIN ANALYSIS FOR LASER RADAR AND COMMUNICATION SYSTEMS

Bernard J. Klein
John J. Degnan

June 1973

Goddard Space Flight Center
Greenbelt, Maryland

PRECEDING PAGE BLANK NOT FILMED

ABSTRACT

The present document is a comprehensive and fairly self-contained study of centrally obscured optical transmitting and receiving antennas and is intended for use by the laser radar and communication systems designer. The material is presented in a format which allows the rapid and accurate evaluation of antenna gain. The Fresnel approximation to scalar wave theory is reviewed and the antenna analysis proceeds in terms of the power gain. Conventional range equations may then be used to calculate the power budget.

The transmitter calculations, resulting in near and far field antenna gain patterns, assumes the antenna is illuminated by a laser operating in the fundamental cavity mode TEM_{00}. A simple equation is derived for matching the incident source distribution to a general antenna configuration for maximum on-axis gain. An interpretation of the resultant gain curves allows a number of auxiliary design curves to be drawn which display the losses in antenna gain due to pointing errors and the cone angle of the outgoing beam as a function of antenna size and central obscuration. The use of telescope defocusing as an approach to spreading the beam for target acquisition is compared to some alternate methods.

Incorporated into the document is an analysis of optical receivers which includes a discussion of the optical losses at the detector. Direct and heterodyne detection schemes are considered separately. Included is a detailed discussion on the manner in which the local oscillator field distribution across the detector affects the overall receiver gain in heterodyne systems.

CONTENTS

LIST OF APPENDICES

TRANSMITTER AND RECEIVER ANTENNA GAIN ANALYSIS FOR LASER RADAR AND COMMUNICATION SYSTEMS

1. INTRODUCTION

Laser communication and tracking systems have long been predicted to have immense capacity to supplement and extend the capabilities of the more conventional microwave and millimeter wave systems. These projections are now being realized in the form of laser tracking systems which have made great advances in the accuracy of orbit determination for both man-made earth satellites and the moon, as well as in the measurement of point-to-point terrestrial distances. Experimental laser communications systems have been developed and systems studies indicate that lasers may represent the optimum approach to transferring high data rates from earth observational spacecraft to NASA's planned Tracking and Data Relay Satellite System (TDRSS). All of these applications share a common analytical base, the range equation for either radar or communications. One of the most important parameters in the range equation is the antenna gain, for both transmitting and receiving antennas. This document had its origin in the recognition that the data available on optical transmitting and receiving antennas was too sparse and incomplete to provide a reasonable and sufficiently accurate basis for system design. In addition, much of the available information was widely scattered among the various scientific and engineering journals and often presented in a format not directly useful to the systems engineer. It became obvious that it would be most desirable to generate a set of comprehensive systems designer-oriented plots which would permit the rapid and convenient determination of transmitting and receiving antenna gain. That has been the authors' objective in writing this document.

Laser communications and radar systems employ conventional telescopes as optical antennas. These telescopes frequently have central obscurations, such as the secondary mirror in the Cassegrainian telescope shown in Fig. 1. It was, therefore, necessary to examine the effects of such obscurations. The narrow beams (i.e., high antenna gains) associated with laser communications and radar systems require precise pointing and the systems designer must be able to relate pointing errors to losses in antenna gain. In addition, the narrow beams, when coupled with the finite velocity of light, necessitate a point-ahead angle which must be considered by the systems designer; this imposes a further requirement that the systems engineer know the distribution of antenna gain with off-axis angle. A knowledge of the antenna gain distribution is of more immediate usefulness than the normalized intensity plots previously recorded by Campbell and DeShazer [1] for the near field and by Buck[2] and Kaufman[3] for the far field.

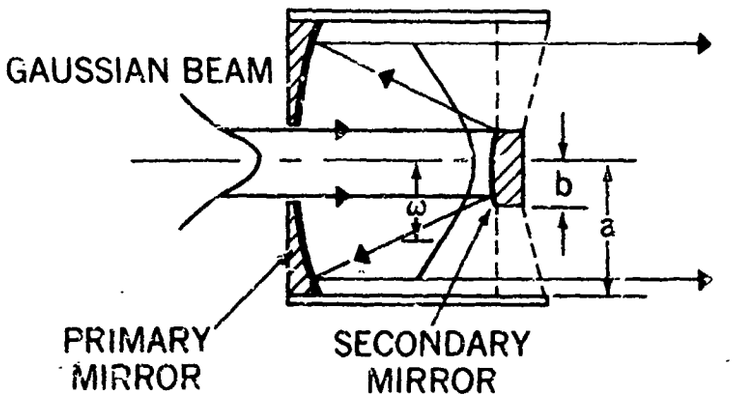

Figure 1. Cassegrainian Telescope

The establishment of communications or tracking in a laser system requires that an acquisition sequence be performed, again because of the narrow beams which are usually much narrower than the angular uncertainties which must be coped with by the system. One approach to acquisition is to utilize a diverged transmitter beam, much wider than the ultimate beamwidth required by bit error rate or tracking accuracy considerations, which is diverged to the maximum extent possible within the limits of the required acquisition signal-to-noise ratio. One means to diverge the transmitter beam is to defocus the optical antenna which effectively transforms the far field pattern to a near field distribution. Defocusing by arbitrary amounts can, however, result in a local intensity minimum on-axis in the far field which may be undesirable for acquisition. Thus, the effect of defocusing must be considered in detail.

In the present document, we review the fundamental assumptions inherent in the Fresnel approximation to scalar wave theory and apply the theory to centrally obscured circular apertures illuminated by Gaussian amplitude wavefronts of varying curvature using a model described in Fig. 1. The beam is characterized by a beam width ω measured from the axis to the $1/e^2$ intensity point and a phase front of curvature R. Both quantities are measured in the plane containing the secondary mirror. The telescope system is described by two parameters, a primary radius "a" and a secondary radius "b". The on-axis power gain is then computed as a function of the various parameters in both the near and far field, and an expression is derived which yields the optimum aperture radius to beam width ratio (a/ω) for maximum on-axis gain in the far field as a function of obscuration ratio (b/a). The off-axis near and far field power gain distributions are then computed for the optimum antenna configurations. A series of auxiliary design curves allow the rapid evaluation of the on or off-axis

gain, the truncation loss by the aperture, and the effective cone angle for an arbitrary wavelength and aperture size. A comparison is made between unapertured laser beams and defocussed antennas when large cone angles are required for acquisition. Finally, the use of centrally obscured antennas as receivers is considered. Calculations of the receiver gain are made which include computations of the losses due to blockage of the light by the central obscuration and its effect on the field distribution at the detector. The losses incurred by systems utilizing direct detection and heterodyne (or homodyne) detection are separately discussed and the procedure for matching the detector dimensions to the telescope system for maximum efficiency is considered in detail.

2. THE FRESNEL DIFFRACTION FORMULATION

In the present analysis, we choose spherical coordinates for the calculation of the field distribution at the point of observation (r_1, θ_1, ϕ_1). Figure 2 shows the diffracting aperture to be in the $\theta_0 = \pi/2$ plane and a point in the aperture designated by the coordinates $(r_0, \pi/2, \phi_0)$.

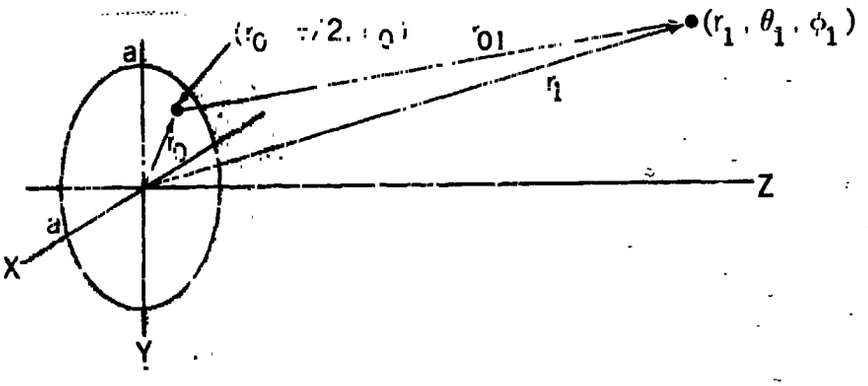

Figure 2. Coordinate System

The distance between points, r_{01}, also shown in Fig.2, is obtained from

$$r_{01}^2 = (x_1 - x_0)^2 + (y_1 - y_0)^2 + (z_1)^2$$

where $z_0 = 0$. In spherical coordinates, the latter expression becomes

$$r_{01}^2 = (r_1 \operatorname{Sin}\theta_1 \operatorname{Cos}\phi_1 - r_0 \operatorname{Cos}\phi_0)^2 + (r_1 \operatorname{Sin}\theta_1 \operatorname{Sin}\phi_1 - r_0 \operatorname{Sin}\phi_0)^2 + (r_1 \operatorname{Cos}\theta_1)^2$$

which reduces to

$$r_{01} = r_1 \left[1 + \frac{r_0^2}{r_1^2} - 2\frac{r_0}{r_1} \operatorname{Sin}\theta_1 \operatorname{Cos}(\phi_1 - \phi_0)\right]^{1/2}$$

The Fresnel approximation assumes that the first two terms of the binomial expansion of the square root are adequate. Thus we have

$$r_{01} = r_1 \left(1 + \frac{r_0^2}{2r_1^2} - \frac{r_0}{r_1} \operatorname{Sin}\theta_1 \operatorname{Cos}(\phi_1 - \phi_0)\right). \tag{1}$$

Huygen's principle states that each point in the aperture is the source of a spherical wave weighted by the amplitude of the field at the point. The electric field at the observation point (r_1, θ_1, ϕ_1) is thus given by an integration over the aperture, that is,[4]

$$E(r_1, \theta_1, \phi_1) = \int_0^a \int_0^{2\pi} \frac{1}{j\lambda r_{01}} e^{jkr_{01}} E_0(r_0, \phi_0)\, d\phi_0\, r_0\, dr_0 \tag{2}$$

where a is the aperture radius, λ is the wavelength, and k is the propagation constant $(2\pi/\lambda)$. If the field distribution at the aperture is circularly symmetric, then Eq. (2) may be written

$$E(r_1, \theta_1, \phi_1) = \frac{1}{j\lambda r_1} e^{jkr_1} \int_0^a \int_0^{2\pi} e^{jkr_0^2/2r_1} E_0(r_0)\, e^{-jk \operatorname{Sin}\theta_1 \operatorname{Cos}(\phi_1 - \phi_0)}\, d\phi_0\, r_0 dr_0 \tag{3}$$

where we have used Eq. (1) to approximate r_{01} in the exponential argument in (2) and the approximation $r_{01} \approx r_1$ in the less critical denominator term. The circular symmetry of our system requires the field at the observation point to be independent of ϕ_1, and we may, therefore, choose a value of ϕ_1 for convenience. Choosing $\phi_1 = -\pi/2$ and using the integral representation of the Bessel function of the first kind given by[5]

$$J_n(z) = \frac{1}{2\pi} \int_0^{2\pi} e^{j(z \sin\phi - n\phi)} d\phi$$

we may write Eq. (3) as

$$E(r_1, \theta_1) = \frac{-jk}{r_1} e^{jkr_1} \int_0^a e^{jkr_0^2/2r_1} J_0(kr_0 \sin\theta_1) E_0(r_0)\, r_0 dr_0. \qquad (4)$$

The latter equation is a valid approximation if the condition

$$\frac{ka^2}{8r_1} \left(\frac{a}{r_1} + 2|\sin\theta_1| \right)^2 << 1$$

is met. The above expression is derived from the third term in the binomial expansion for r_{01} and sets limits on the observation regions for which the Fresnel approximation is valid.

3. TRANSMITTER GAIN

3.1 Definition of the Optical Antenna Gain

We assume the incident source function $E_0(r_0)$ to have a Gaussian amplitude function (corresponding to the fundamental laser mode) and to be given by the equation

$$E_0(r_0) = \sqrt{\frac{2}{\pi\omega^2}}\, e^{-r_0^2/\omega^2}\, e^{jkr_0^2/2R}$$

where ω is the distance from the axis to the $1/e^2$ intensity point and R is the curvature of the phase front at the aperture (See Appendix A). The proportionality constant normalizes the incident power P over the entire aperture plane to one, i.e.,

$$P = \int_0^{2\pi} \int_0^{\infty} |E_0(r_0)|^2\, r_0 dr_0 d\phi_0 \qquad (5)$$

1.

We assume this field function $E_0(r_0)$ to impinge upon a centrally obscured aperture having an opaque obscuring element of radius b. The impinging field is centered about the telescope axis. Axicon devices and off-axis incident fields will not be considered in the present work. The latter approaches attempt to redistribute the field in order to minimize the obscuration by the secondary mirror and the resultant degradation in transmitted power. Peters and Ledger[6] consider axicon devices in great detail and note the advantage in particular for an obscuration ratio (b/a) of 0.5. This central obscuration to aperture ratio is larger than is commonly employed. For smaller b/a values, the improvement in on-axis gain is marginal and does not appear to justify the more stringent alignment tolerances.[7]

With the substitution of $E_0(r_0)$ in Eq. (4), the intensity[8] distribution at the observation point (r_1, θ_1) is given by

$$I(r_1, \theta) = \frac{k^2}{r_1^2}\left|\int_b^a \frac{\sqrt{2}}{\sqrt{\pi}\omega} e^{-r_0^2/\omega^2} e^{j\frac{kr_0^2}{2}\left(\frac{1}{r_1}+\frac{1}{R}\right)} J_0(kr_0 \operatorname{Sin}\theta_1)\, r_0\, dr_0\right|^2 . \tag{6}$$

The intensity of the radiation field produced at a distance r_1 from a unit power isotropic radiator is, of course, given by

$$I_0 = \frac{1}{4\pi r_1^2}$$

In the ensuing calculations, we choose to define the gain by the expression

$$G(r_1, \theta_1) = \frac{I(r_1, \theta_1)}{I_0}$$

$$= \frac{8k^2}{\omega^2}\left|\int_b^a e^{j\frac{kr_0^2}{2}\left(\frac{1}{r_1}+\frac{1}{R}\right)} e^{-r_0^2/\omega^2} J_0(kr_0 \operatorname{Sin}\theta_1)\, r_0\, dr_0\right|^2 \tag{7}$$

where the gain depends on r_1 only in the near field.

It is important to note that the above definition of gain differs from the definition conventionally used in microwave theory[9] in that the power of the isotropic radiator is set equal to the total power (unity) impinging on the aperture plane as opposed to the power actually transmitted by the aperture. The latter is given by

$$P = \frac{2}{\pi\omega^2}\int_0^{2\pi}\int_b^a e^{-2\,r_0^2/\omega^2}\, r_0\, dr_0\, d\phi_0$$

$$= e^{-2b^2/\omega^2} - e^{-2a^2/\omega^2} \leq 1.$$

Thus, the gain calculated under the present definition will be smaller by the factor $(e^{-2\alpha^2\gamma^2} - e^{-2\alpha^2})$ where $\alpha = a/\omega$ and $\gamma = b/a$. Our choice of definition is motivated by the fact that, for the systems presently under discussion, truncation by the aperture boundary and obscuration by the secondary represent real losses in transmitter power and hence should be included in a calculation of the overall antenna gain. From the conventional definition of gain, we would obtain the result that $a/\omega \to 0$ (uniform illumination) is optimum for maximum on-axis gain in the far field. This is a realistic result only if all of the available energy is actually transmitted by the aperture. Therefore, the conventional definition might be appropriate for systems where the energy is redistributed by means of an axicon or other device; it is not appropriate for the systems presently under discussion.

The qualitative behavior of the curves in Fig. 3 can be explained quite easily. As a very large spot size ω is made smaller relative to the aperture radius (a/ω increasing), less energy is lost due to truncation and the fractional power transmitted increases. For centrally obscured antennas ($\gamma \neq 0$), however, a further reduction in the spot size results in a significant fraction being blocked by the secondary with the net result that the curves corresponding to obscured apertures exhibit a minimum loss point. As we shall see later, however, the a/ω ratios corresponding to maximum fractional transmission by the aperture do not coincide with those values which give the maximum on-axis gain.

Returning to Eq. (7) we make a substitution of $r_0 = s \cdot a$, where s is a dimensionless variable and a is the aperture radius, and obtain

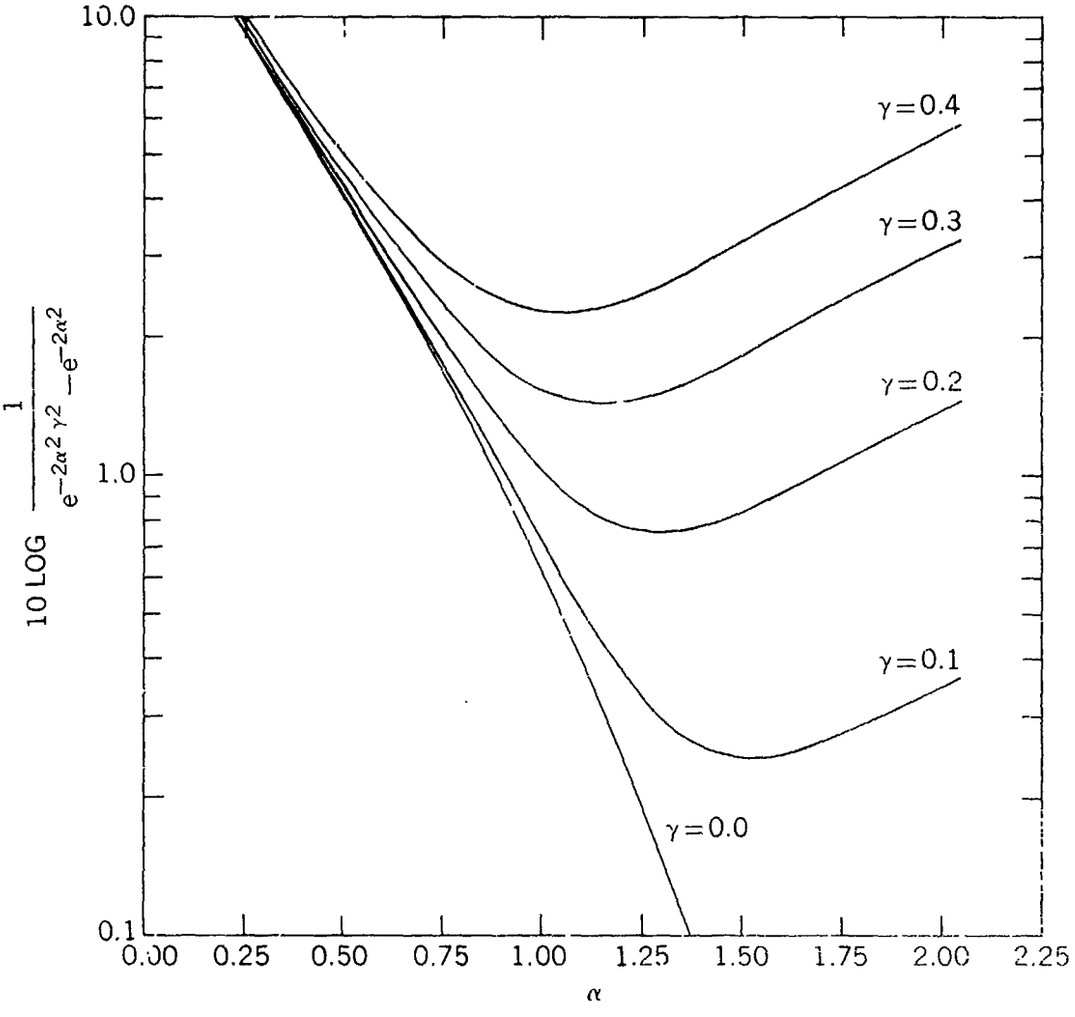

Figure 3. Combined truncation and obscuration loss in dB

$$G(r_1, \vartheta_1) = \frac{8k^2}{\omega^2}\left|\int_{b/a}^{1} e^{j\frac{ka^2}{2}\left(\frac{1}{r_1}+\frac{1}{R}\right)s^2} e^{-\frac{a^2}{\omega^2}s^2} J_0(ka\,\mathrm{Sin}\vartheta_1\, s)\, a^2\, s\, ds\right|^2. \qquad (8)$$

We now define a number of dimensionless parameters to simplify Eq. (8) and rewrite it as

$$G_T(\alpha, \beta, \gamma, X) = 8\left(\frac{4\pi^2}{\lambda^2}\right)a^2\alpha^2\left|\int_{\gamma^2}^{1} e^{j\beta u} e^{-\alpha^2 u} J_0(X\sqrt{u})\,\frac{1}{2}\,du\right|^2 \qquad (9)$$

where we have defined

$$\left.\begin{aligned} u &= s^2 \\ \alpha &= a/\omega \\ \gamma &= b/a \\ X &= ka \sin \theta_1 \\ \beta &= \frac{ka^2}{2}\left(\frac{1}{r_1} + \frac{1}{R}\right). \end{aligned}\right\} \tag{10}$$

Eq. 9 can be rewritten as

$$G_T(\alpha, \beta, \gamma, X) = \frac{4\pi A}{\lambda^2} \cdot g_T(\alpha, \beta, \gamma, X) \tag{11}$$

where α and γ are system parameters $X = ka \sin \theta$, is a convenient plotting parameter for off-axis distributions, β includes near field and defocusing effects and $A = \pi a^2$ is the aperture area. The factor $4\pi A/\lambda^2$ is the well known upper limit on antenna gain which is obtained for a uniformly illuminated unobscured circular aperture.[9]

In the following sections, we examine the function $g(\alpha, \beta, \gamma, X)$ which we shall refer to as the "transmitter efficiency factor" and which is defined by the equation

$$g_T(\alpha, \beta, \gamma, X) = 2\alpha^2 \left| \int_{\gamma^2}^{1} e^{j\beta u} e^{-\alpha^2 u} J_0(X\sqrt{u})\, du \right|^2 . \tag{12}$$

3.2 On-Axis Gain

A general equation for the on-axis antenna efficiency for incident Gaussian energy may be obtained by setting $X = 0$ in Eq. (12) and performing the rather simple integration to obtain

$$g_T(\alpha, \beta, \gamma, 0) = \left(\frac{2\alpha^2}{\beta^2 + \alpha^4}\right)\left\{e^{-2\alpha^2} + e^{-2\alpha^2\gamma^2} - 2e^{-\alpha^2(\gamma^2+1)}\cos[\beta(\gamma^2-1)]\right\} \quad (13)$$

If we specialize to the far field and Gaussian amplitude plane waves ($\beta = 0$) impinging on an unobscured aperture ($\gamma = 0$), Eq. (13) becomes

$$g_T(\alpha, 0, 0, 0) = \frac{2}{\alpha^2}\left[e^{-\alpha^2} - 1\right]^2. \quad (14)$$

Setting the derivative of Eq. (14) equal to zero yields the transcendental equation

$$[2\alpha_0^2 + 1]\cdot e^{-\alpha_0^2} = 1 \quad (15)$$

which can be solved numerically or graphically to obtain $\alpha_0 = 1.12$ for the aperture to spot size ratio that yields the maximum on-axis gain for the unobscured case. The corresponding value of the efficiency factor is equal to 0.8145.

For a non-zero obscuration ratio, Eq. (13) becomes

$$g_T(\alpha, 0, \gamma, 0) = \frac{2}{\alpha^2}\left[e^{-\alpha^2} - e^{-\gamma^2\alpha^2}\right]^2. \quad (16)$$

If we take the derivative with respect to α, we again obtain a transcendental equation, that is

$$\frac{2\alpha^2 + 1}{2\alpha^2\gamma^2 + 1}\, e^{-\alpha^2(1-\gamma^2)} = 1 \quad (17)$$

An approximate solution obtained using second order perturbation theory (See Appendix B) is given by

$$\alpha \approx 1.12 - 1.30\gamma^2 + 2.12\gamma^4. \quad (18)$$

Eq. (18) gives the optimum aperture to beam width ratio for a general obscuration and is accurate to within ±1% for $\gamma \leq 0.4$.

Figure 4 illustrates the degradation in the far field efficiency factor experienced when non-optimum antenna configurations are used. Each curve is labeled by a particular value of obscuration ratio γ, and the efficiency factor is plotted (in dB) versus the aperture radius to beam width ratio.

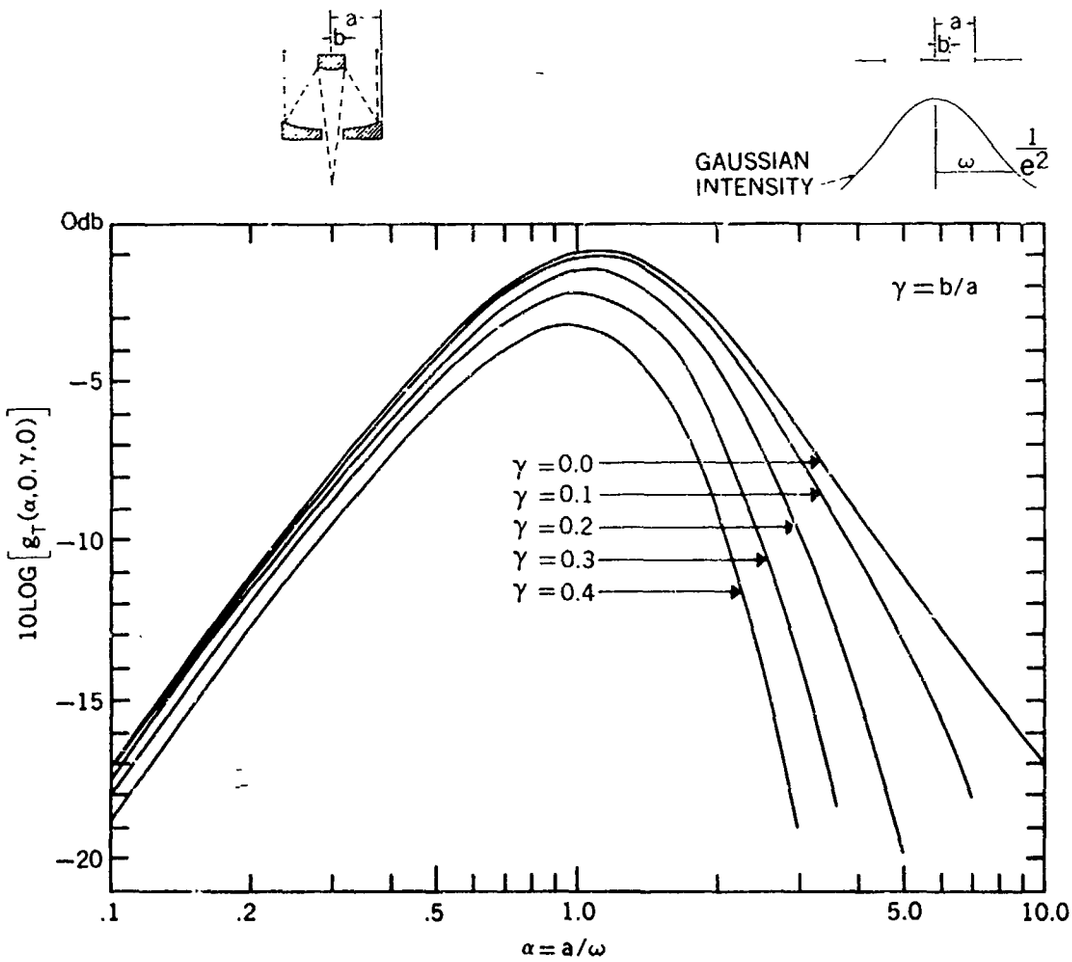

Figure 4. Far field axial gain relative to $4\pi A/\lambda^2$ as a function of α for five different obscuration ratios (γ)

We now consider the on-axis gain in the near field for the optimum antennas just derived. This can be obtained by choosing a particular value for γ, calculating the corresponding value of α from Eq. (18), substituting both values into Eq. (13)

and plotting the efficiency factor versus β. Figure 5, where we have chosen to plot $10 \operatorname{Log} g(\alpha, \beta, \gamma, 0)$ versus $\beta/2\pi$, clearly displays a series of gain minima. As we shall see in the next section, these minima correspond to observation regions where a local intensity minimum (shadow) occurs on-axis in the gain profile. It is worthwhile to note that the minima occur for unobscured as well as obscured antennas and, therefore, are not related to the shadow produced by the secondary mirror. Instead they result from destructive interference between the Huygens wavelets. Their positions correspond approximately to the well-known intensity nulls which are observed at discrete distances (integer values of $\beta/2\pi$) from a uniformly illuminated aperture.[1] In the case of uniform illumination, the cancellation of electric field is total; Gaussian illumination produces only partial cancellation. In addition, the positions of the minima are displaced slightly in going from a uniform to a Gaussian distribution. Increasing the obscuration ratio from zero displaces the minima toward larger values of β.

For plane waves incident on the aperture, the far field value of the on-axis efficiency factor is, of course, the value at $\beta = 0$. As the distance between the aperture and the observation plane decreases, β increases. From our definition for β, however, other information is obtainable from Fig. 5. The effect of phase front curvature at the aperture on the efficiency factor in either the near or far field can be determined by calculating the appropriate value for β (including both near field and phase curvature terms as given by equation (10)) and reading the corresponding efficiency factor from Fig. 5. Thus, Fig. 5 is a concise method for describing an infinite number of experimental situations.

3.3 Antenna Gain Patterns

We now turn our attention to the off-axis gain ($\theta \neq 0$). Figures 6 through 10 are computer generated plots of the transmitter efficiency factor given by Eq. (12). Details pertaining to the numerical techniques employed in the calculation are included in Appendix C as is a complete listing of the computer program. Each figure assumes specific values for γ and α. The latter parameter is calculated from Eq. (18) for maximum axial gain in the far field. The curves displayed within each figure are labeled by the appropriate values of $\beta/2\pi$. In part (a) of Figures 6 through 10 values of $\beta/2\pi$ were chosen corresponding to values midway between adjacent extrema (maxima and minima) in Fig. 5. In part (b), β values corresponding to the first few extrema in Fig. 5 are considered. Comparing Figs. 6 through 10 with Fig. 5 verifies the assertion made in the previous section that the minima in Fig. 5 correspond to local intensity minima on-axis ("shadows" in the central lobe). The maxima in Fig. 5, on the other hand, are associated with localized enhancement of the gain near the axis.

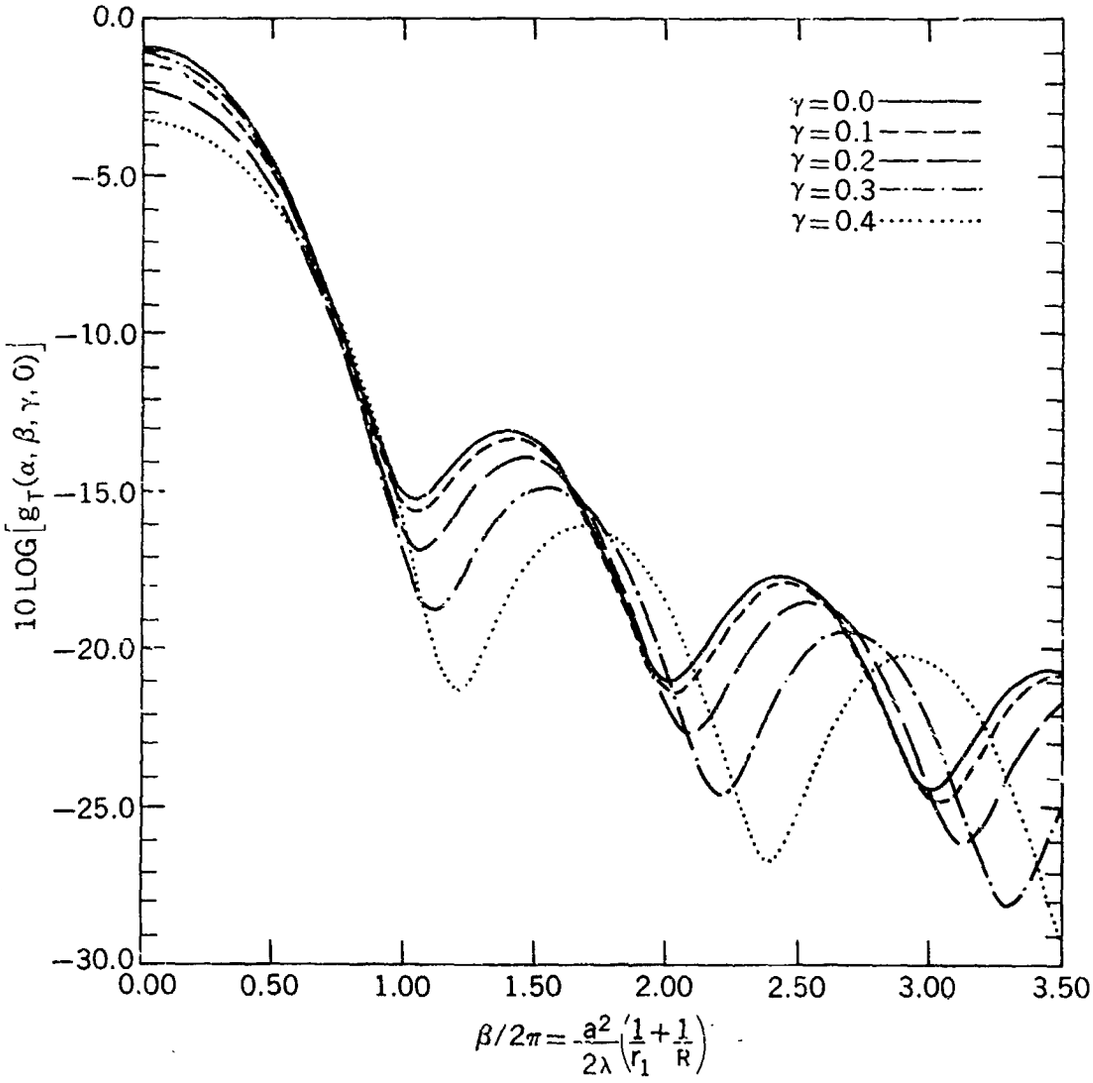

Figure 5. Axial gain relative to $4\pi A/\lambda^2$ as one proceeds from the far field ($\beta = 0$) to the near field ($\beta \neq 0$) for four different obscuration ratios. The same curve can be used to determine the degradation in the far field gain due to defocusing (see eq. (10) in the text). The minima correspond to shadows in the central lobe of the antenna pattern. These shadows occur at certain distances from the aperture in the near field and also in the far field when the system is sufficiently defocused.

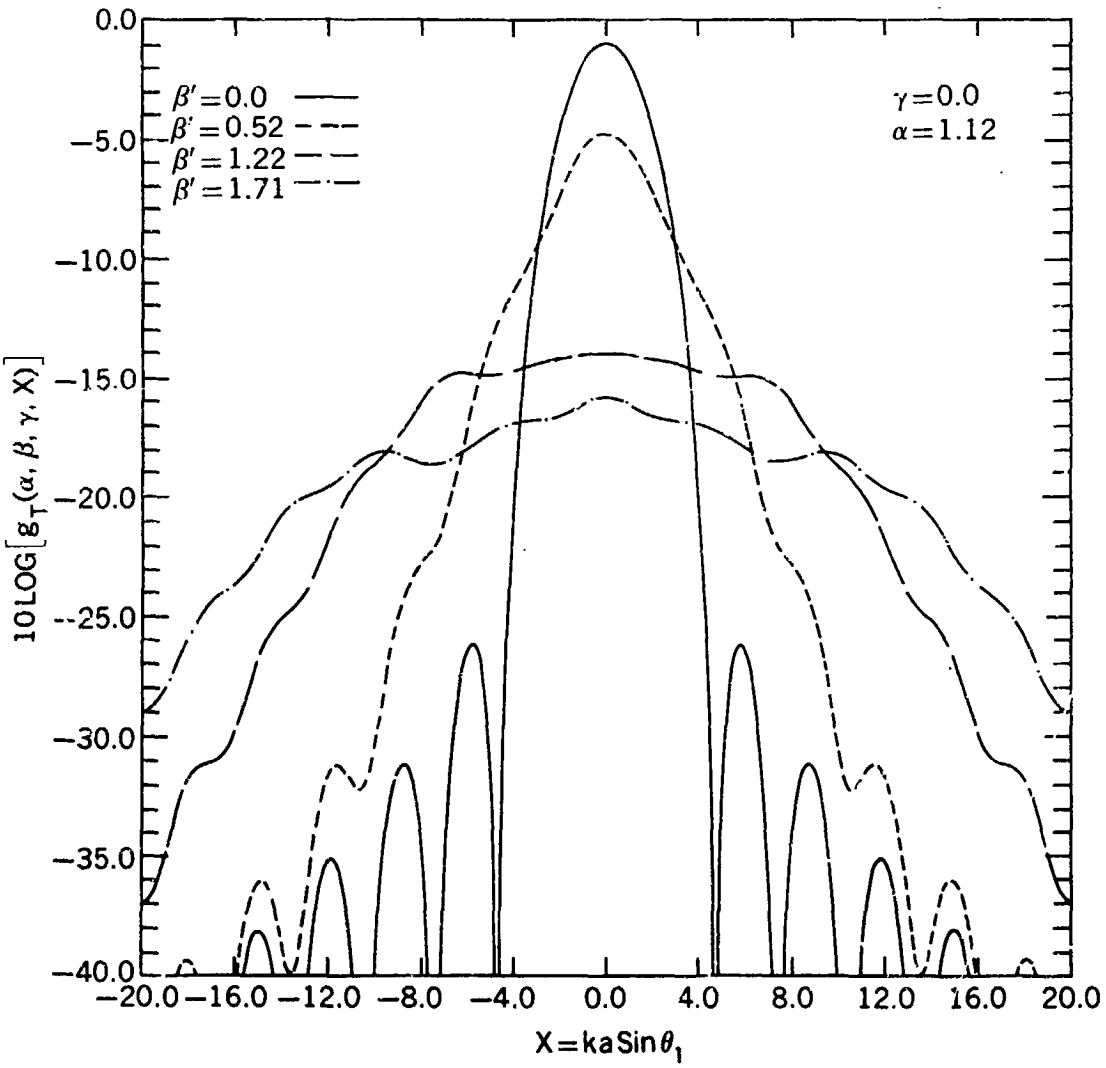

Figure 6a. Far field ($\beta = 0$) and near field ($\beta \neq 0$) transmitting antenna gain distributions in dB relative to $4\pi A/\lambda^2$ as a function of the angle θ, from the optical axis of the antenna. The aperture to gaussian spot size ratio α is chosen to give maximum on-axis gain in the far field according to Eq. (18) in the text. The near field plots are labeled by the value $\beta' = \beta/2\pi$ and also correspond to far field gain distributions obtained from defocused antennas.

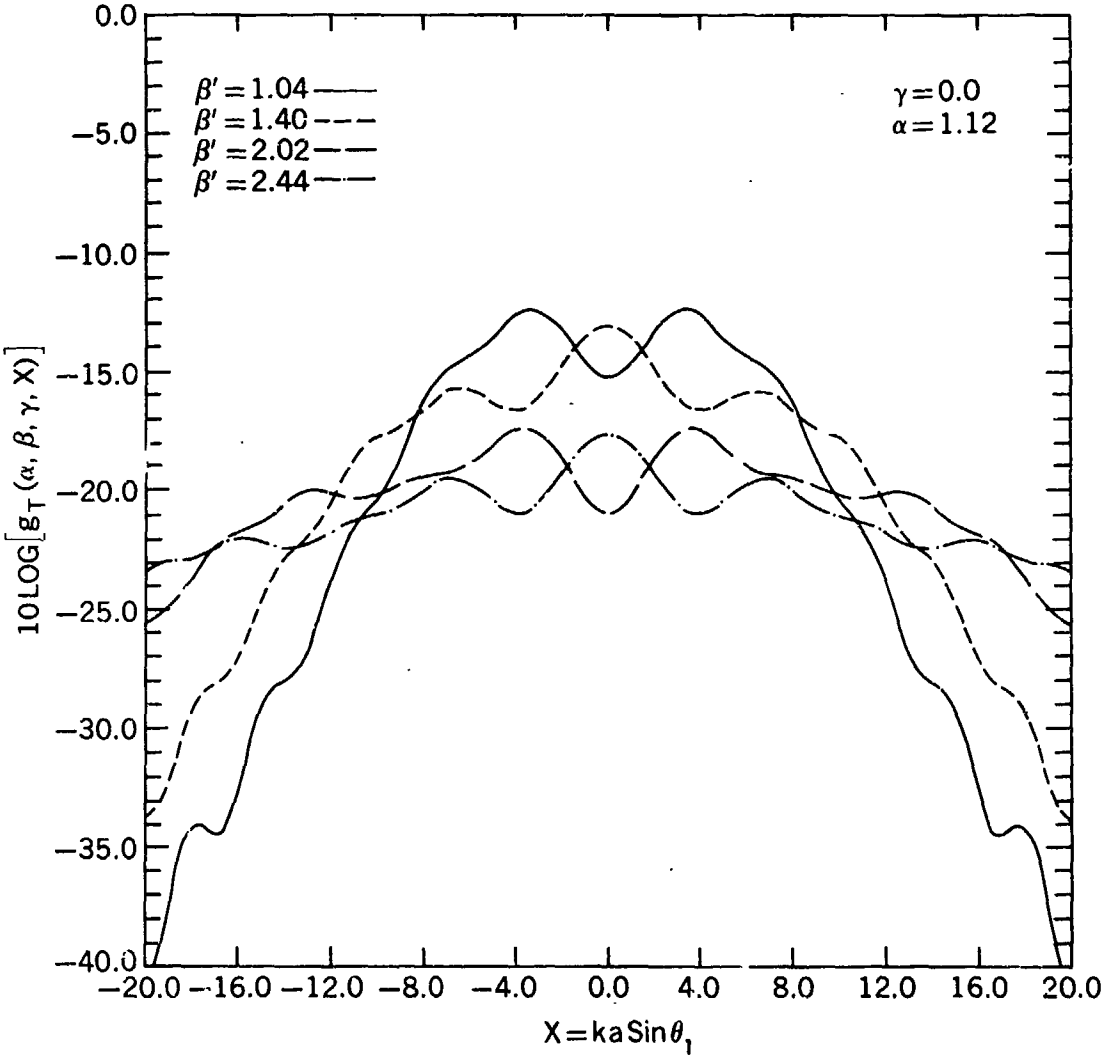

Figure 6b. Near field (or defocused far field) transmitting antenna gain distributions in dB relative to $4\pi A/\lambda^2$ as a function of the angle θ, from the optical axis of the antenna. The aperture to gaussian spot size ratio α is chosen to give maximum on-axis gain in the far field according to Eq. (18) in the text. The near field plots are labeled by the values $\beta' = \beta/2\pi$ corresponding to the maxima and minima in Fig. (5). Comparisons with the latter figure indicate that the minima in Fig. (5) correspond to on-axis shadows in the central lobe and that the maxima correspond to localized enhancements of the on-axis gain.

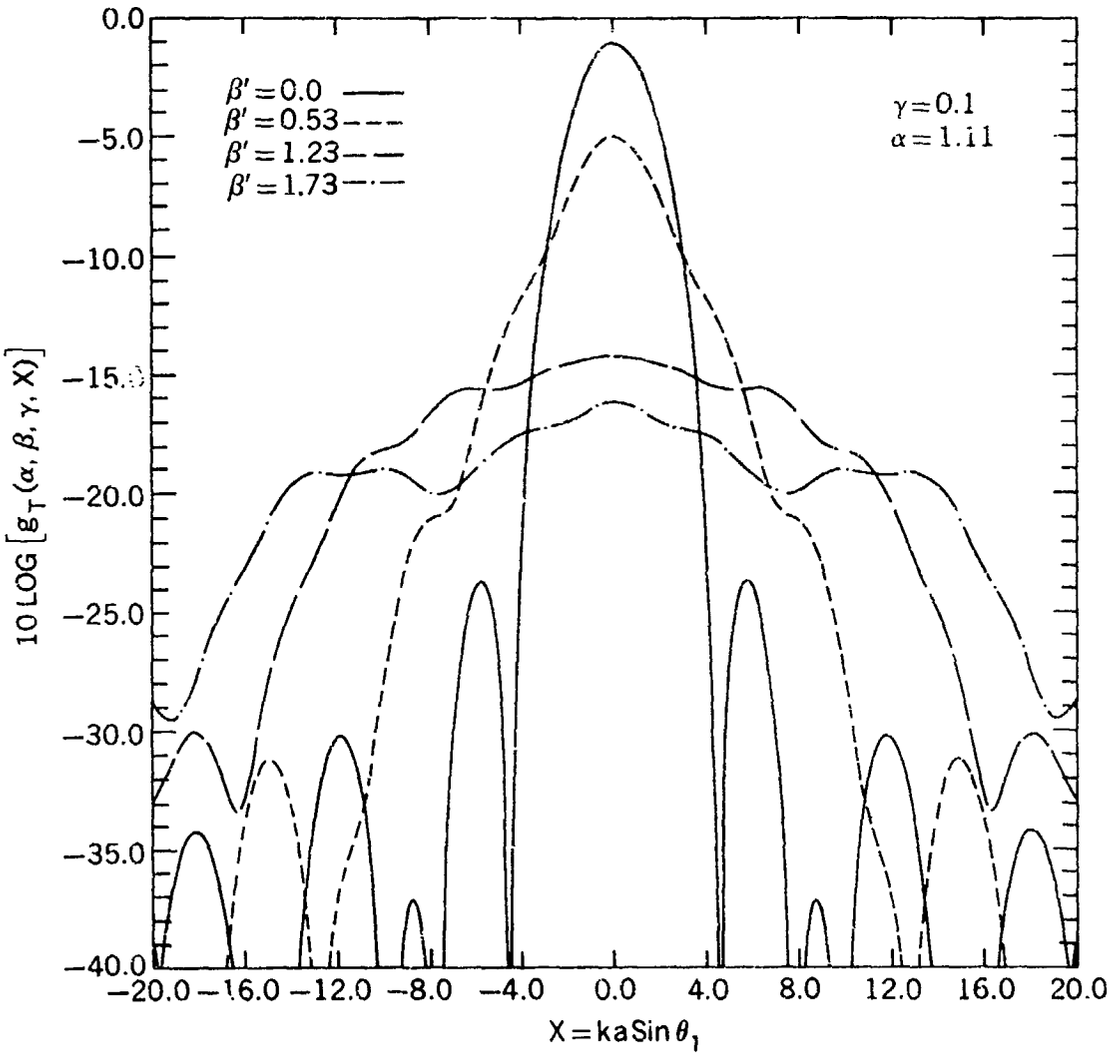

Figure 7a. Far field ($\beta = 0$) and near field ($\beta \neq 0$) transmitting antenna gain distributions in dB relative to $4\pi A/\lambda^2$ as a function of the angle θ, from the optical axis of the antenna. The aperture to gaussian spot size ratio α is chosen to give maximum on-axis gain in the far field according to Eq. (18) in the text. The near field plots are labeled by the value $\beta' = \beta/2\pi$ and also correspond to far field gain distributions obtained from defocused antennas.

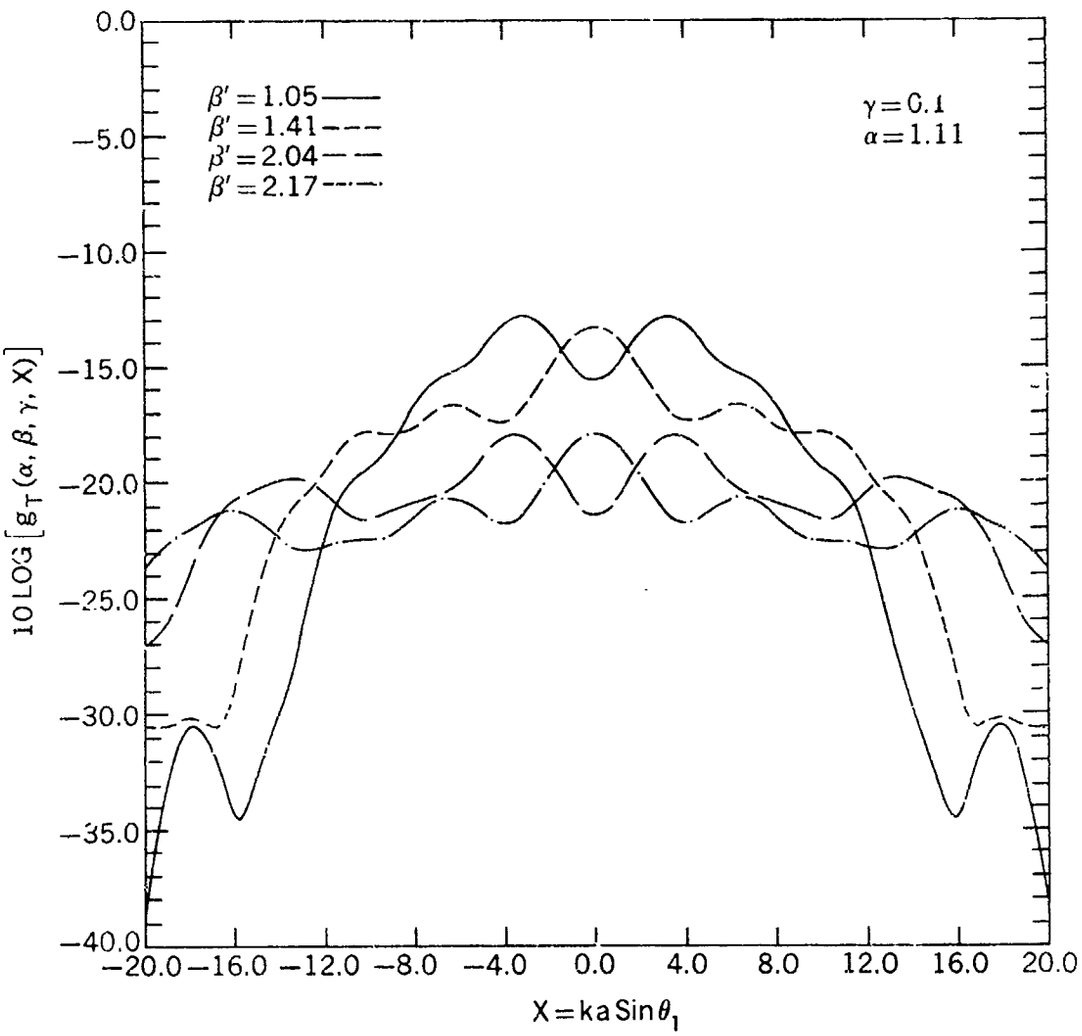

Figure 7b. Near field (or defocused far field) transmitting antenna gain distributions in dB relative to $4\pi A_r/\lambda^2$ as a function of the angle θ_1 from the optical axis of the antenna. The aperture to gaussian spot size ratio α is chosen to give maximum on-axis gain in the far field according to Eq. (18) in the text. The near field plots are labeled by the values $\beta' = \beta/2\pi$ corresponding to the maxima and minima in Fig. (5). Comparisons with the latter figure indicate that the minima in Fig. (5) correspond to on-axis shadows in the central lobe and that the maxima correspond to localized enhancements of the on-axis gain.

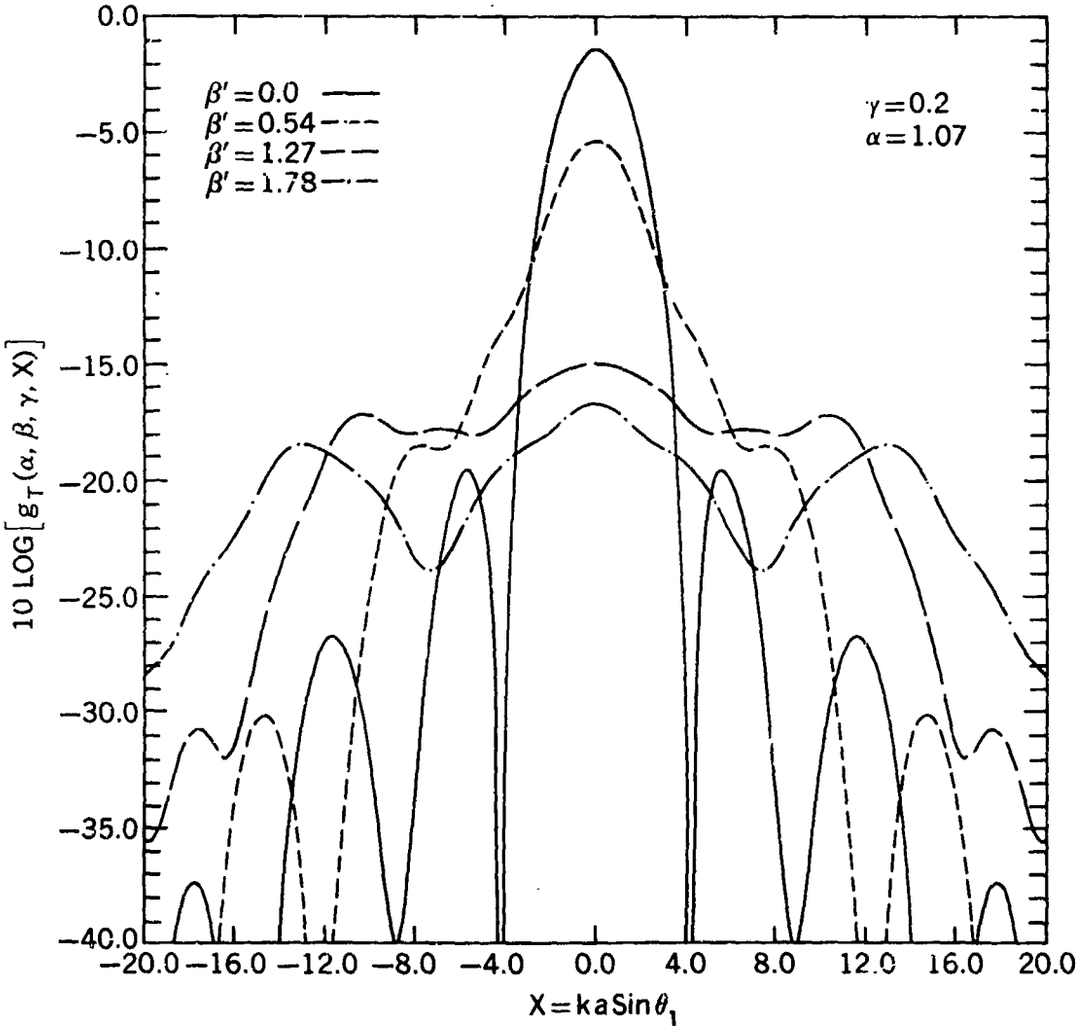

Figure 8a. Far field ($\beta = 0$) and near field ($\beta \neq 0$) transmitting antenna gain distributions in dB relative to $4\pi A/\lambda^2$ as a function of the angle θ, from the optical axis of the antenna. The aperture to gaussian spot size ratio α is chosen to give maximum on-axis gain in the far field according to Eq. (18) in the text. The near field plots are labeled by the value $\beta' = \beta/2\pi$ and also correspond to far field gain distributions obtained from defocused antennas.

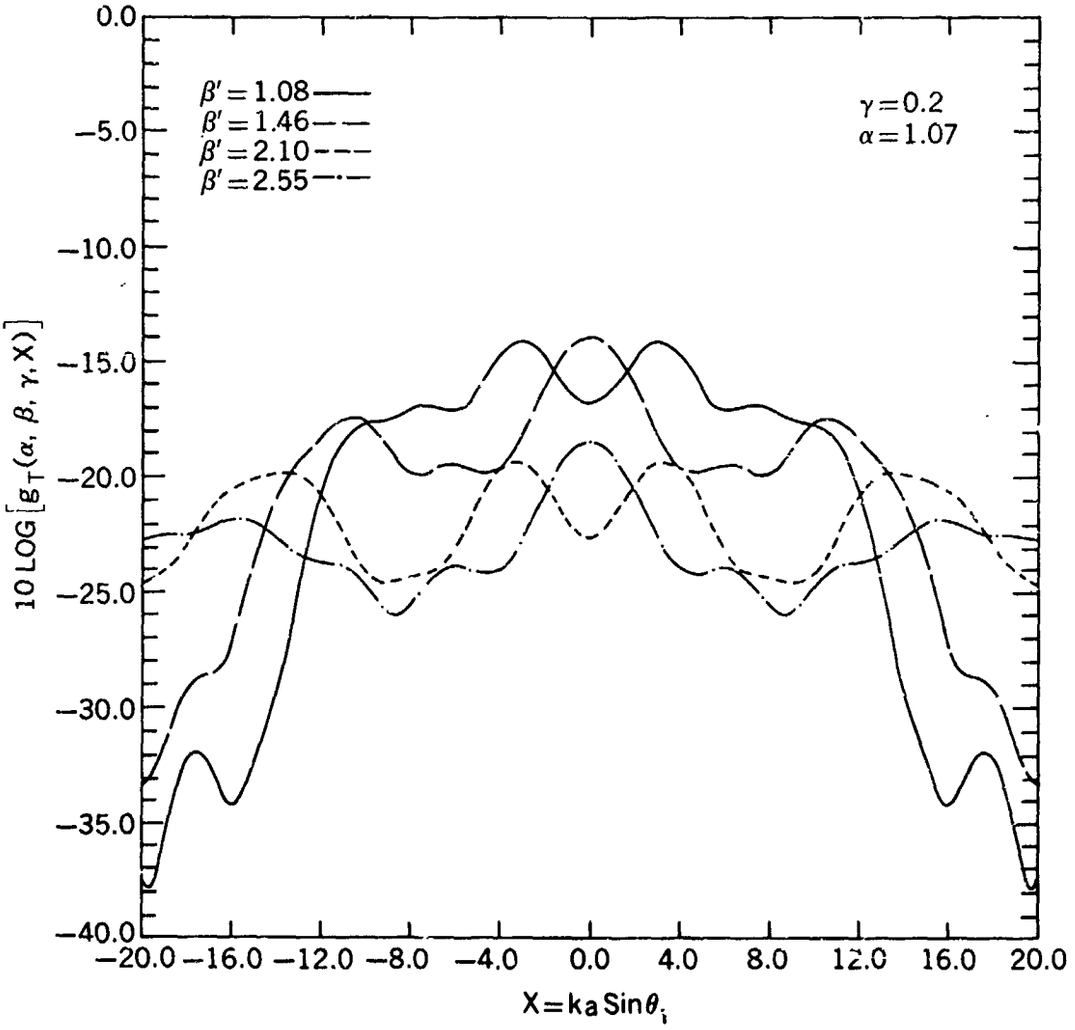

Figure 8b. Near field (or defocused far field) transmitting antenna gain distributions in dB relative to $4\pi A/\lambda^2$ as a function of the angle θ_i from the optical axis of the antenna. The aperture to gaussian spot size ratio α is chosen to give maximum on-axis gain in the far field according to Eq. (18) in the text. The near field plots are labeled by the values $\beta' = \beta/2\pi$ corresponding to the maxima and minima in Fig. (5). Comparisons with the latter figure indicate that the minima in Fig. (5) correspond to on-axis shadows in the central lobe and that the maxima correspond to localized enhancements of the on-axis gain.

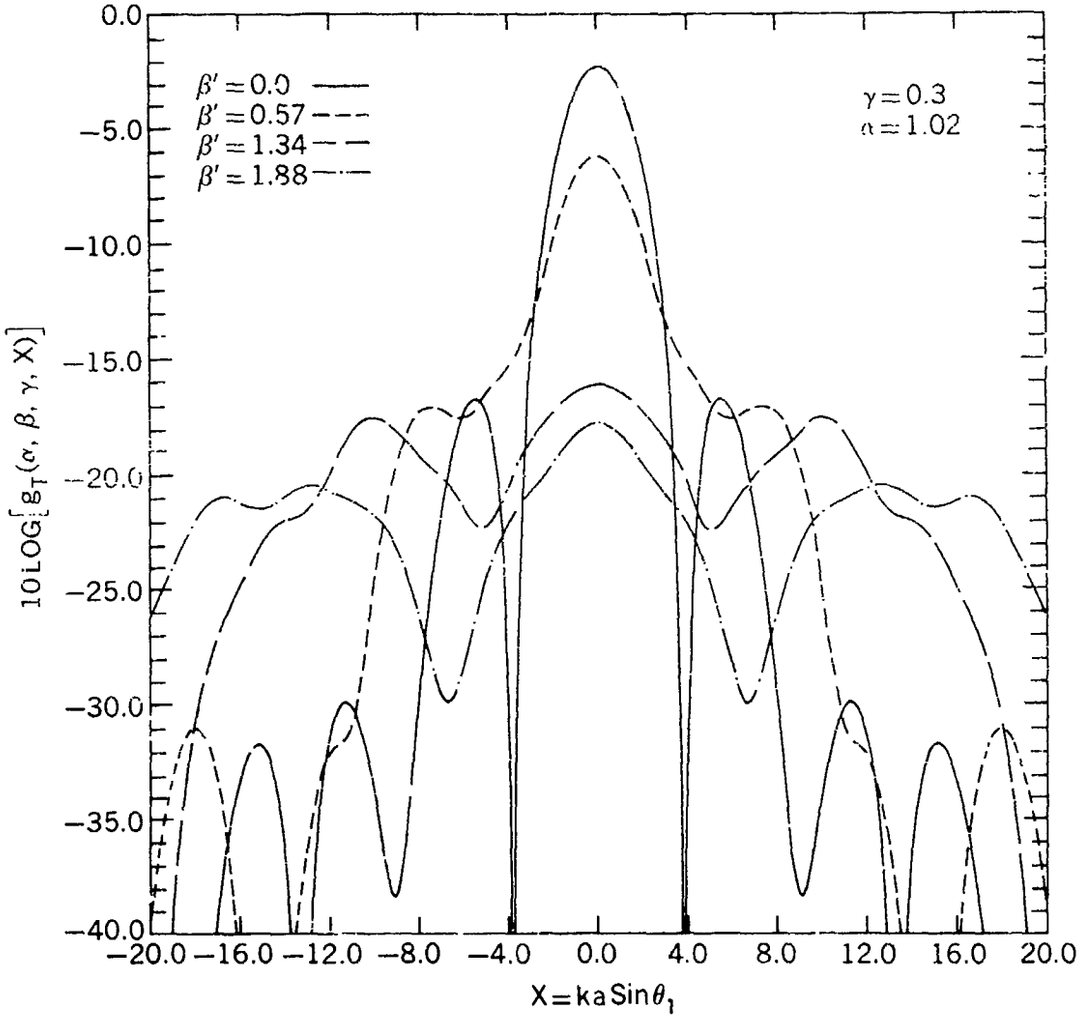

Figure 9a. Far field ($\beta = 0$) and near field ($\beta \neq 0$) transmitting antenna gain distributions in dB relative to $4\pi A/\lambda^2$ as a function of the angle θ, from the optical axis of the antenna. The aperture to gaussian spot size ratio α is chosen to give maximum on-axis gain in the far field according to Eq. (18) in the text. The near field plots are labeled by the value $\beta' = \beta/2\pi$ and also correspond to far field gain distributions obtained from defocused antennas.

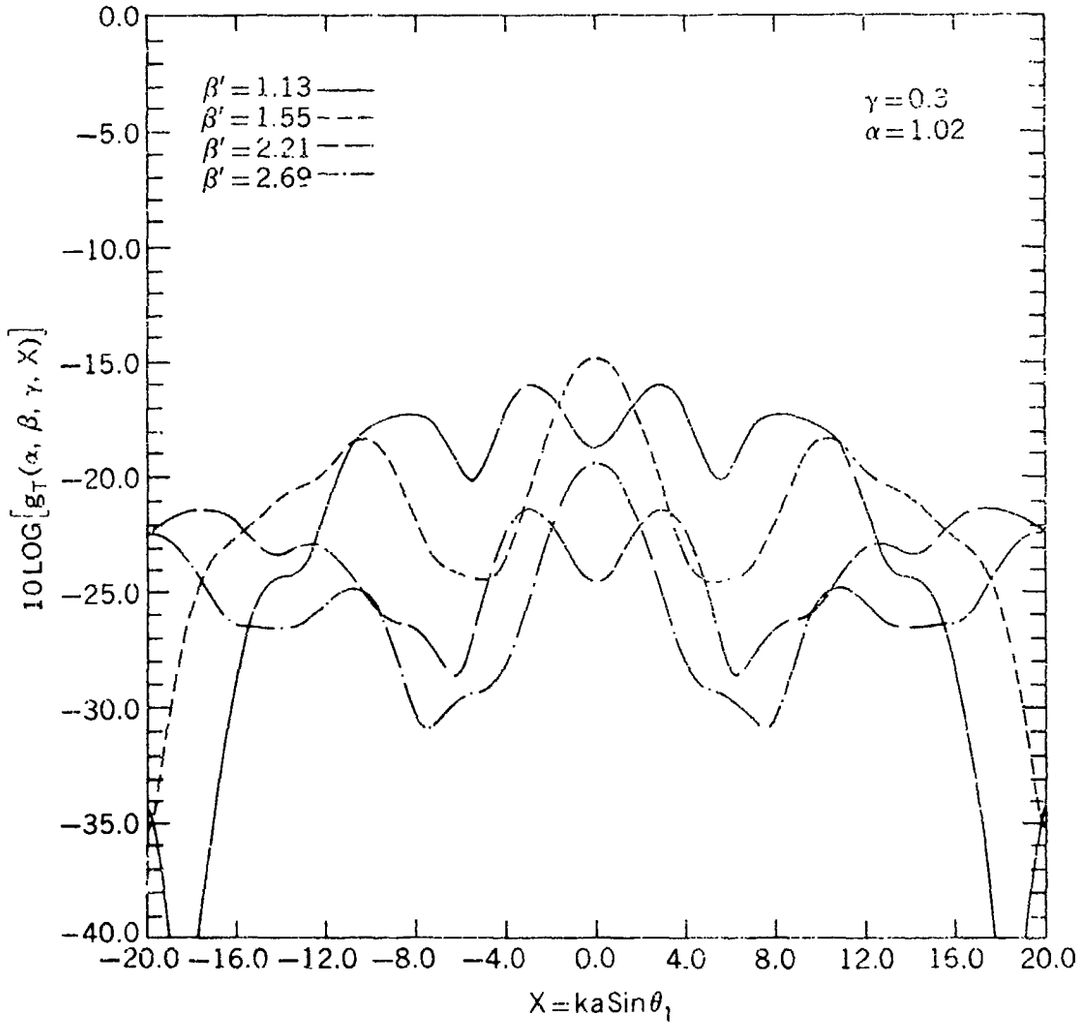

Figure 9b. Near field (or defocused far field) transmitting antenna gain distributions in dB relative to $4\pi A_r/\lambda^2$ as a function of the angle θ_1 from the optical axis of the antenna. The aperture to gaussian spot size ratio α is chosen to give maximum on-axis gain in the far field according to Eq. (18) in the text. The near field plots are labeled by the values $\beta' = \beta/2\pi$ corresponding to the maxima and minima in Fig. (5). Comparisons with the latter figure indicate that the minima in Fig. (5) correspond to on-axis shadows in the central lobe and that the maxima correspond to localized enhancements of the on-axis gain.

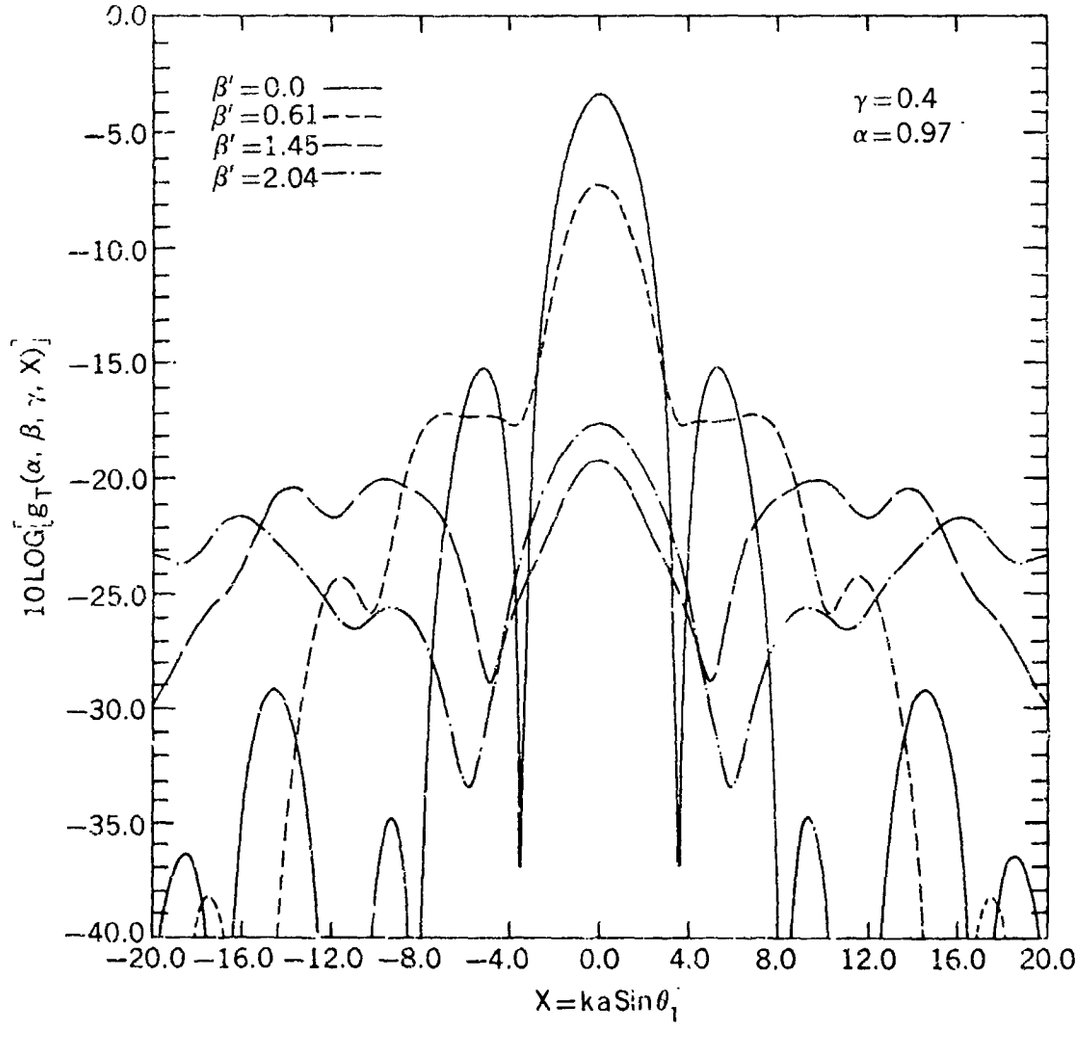

Figure 10a. Far field ($\beta = 0$) and near field ($\beta \neq 0$) transmitting antenna gain distributions in dB relative to $4\pi A/\lambda^2$ as a function of the angle θ_1 from the optical axis of the antenna. The aperture to gaussian spot size ratio α is chosen to give maximum on-axis gain in the far field according to Eq. (18) in the text. The near field plots are labeled by the value $\beta' = \beta/2\pi$ and also correspond to far field gain distributions obtained from defocused antennas.

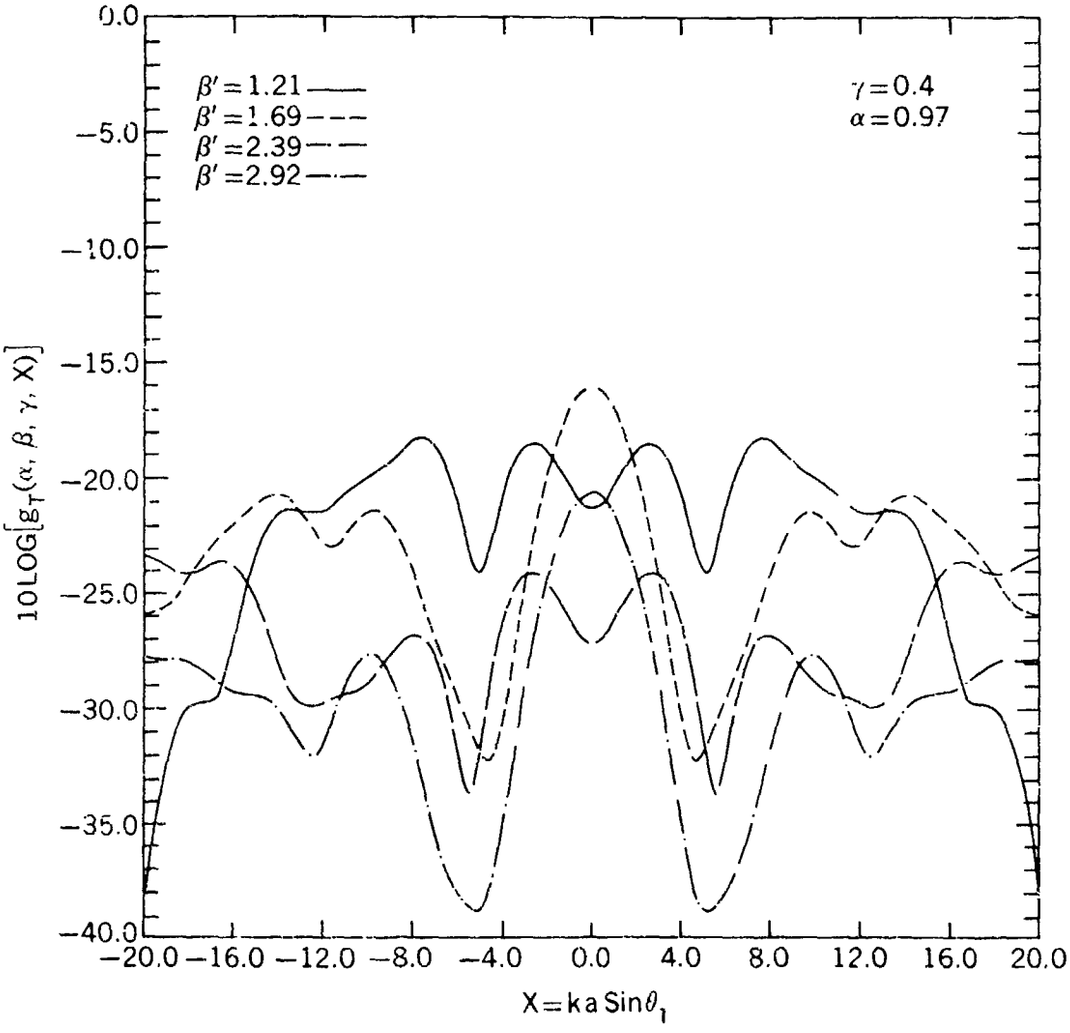

Figure 10b. Near field (or defocused far field) transmitting antenna gain distributions in dB relative to $4\pi A/\lambda^2$ as a function of the angle θ_1 from the optical axis of the antenna. The aperture to gaussian spot size ratio α is chosen to give maximum on-axis gain in the far field according to Eq. (18) in the text. The near field plots are labeled by the values $\beta' = \beta/2\pi$ corresponding to the maxima and minima in Fig. (5). Comparisons with the latter figure indicate that the minima in Fig. (5) correspond to on-axis shadows in the central lobe and that the maxima correspond to localized enhancements of the on-axis gain.

In all the curves, the efficiency factor is plotted against the dimensionless parameter X = ka Sin θ_1. This is a particularly useful format since the spreading of the beam in the far field and the dependence of the cone angle on aperture size is automatically taken into account. This eliminates cumbersome scale transformations in going from one observation distance to another or to different aperture sizes or wavelengths.

3.4 Transmitter Summary

It is now possible to generate several useful curves which greatly simplify the evaluation of optical antennas for a particular application. From Eq. (11), the transmitter gain in dB for a general antenna at an arbitrary observation point is given by

$$G_T(db) = 10 \cdot \mathrm{Log}\left(\frac{4\pi A}{\lambda^2}\right) + 10 \cdot \mathrm{Log}[g_T(\alpha, \beta, \gamma, X)] \tag{19}$$

The first term of Eq. (19) is plotted in Fig. 11 for several important wavelengths as a function of aperture radius. The second term, corresponding to the efficiency factor in dB, is a function of four variables. The on-axis (X = 0) efficiency factor for optimized focused systems (α given by Eq. (18)) in the far field (β = 0) is plotted versus γ in Fig. 12. Near field or defocusing effects ($\beta \neq 0$) on the efficiency factor for these optimized antennas can be estimated reasonably well using Fig. 5. Far field efficiency factors for arbitrary non-optimum antenna structures can be obtained from Fig. 4.

The off-axis ($X \neq 0$) gain normalized to the on-axis gain is displayed in Fig. 13 for four optimized antennas corresponding to γ = 0.0, 0.2, 0.3, and 0.4. These curves indicate the dB loss in far field gain attributed to pointing error and are plotted versus the angular error θ in units of λ/D radians where D is the antenna aperture diameter. Fig. 13 can in turn be used to define the cone angle of the outgoing beam. If we choose to define the half angle of the cone, θ_1, as the angle from the optical axis to the $1/e^2$ point on the power gain distribution (Fig. 13), we obtain the curves presented in Fig. 14. In the latter figure, each shaded region is associated with its corresponding laser wavelength. For a given aperture radius, the upper and lower limits of the shaded regions are defined (somewhat arbitrarily) by the angular spread of the optimized antennas for the unobscured case [θ_1 (γ = 0.0) = 0.94 λ/D] and for an obscuration ratio of 0.4 [θ_1 (γ = 0.4) = 0.79 λ/D] respectively where the latter relations were obtained from the -8.7 dB ($1/e^2$) points in Fig. 13. One can interpolate between these two limits to obtain cone half-angles for intermediate values of γ.

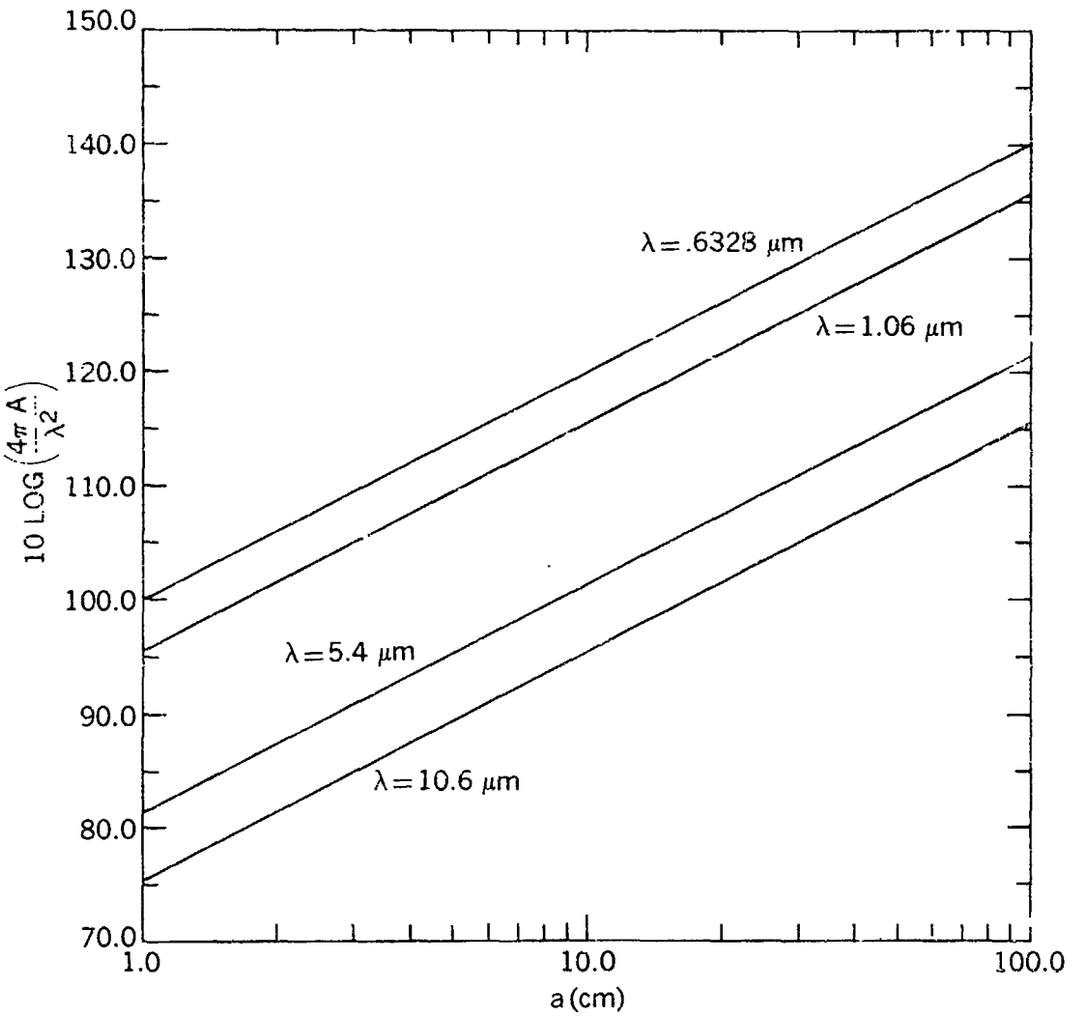

Figure 11. The maximum theoretical gain ($4\pi A/\lambda^2$) available from a circular aperture of radius a for several important laser wavelengths.

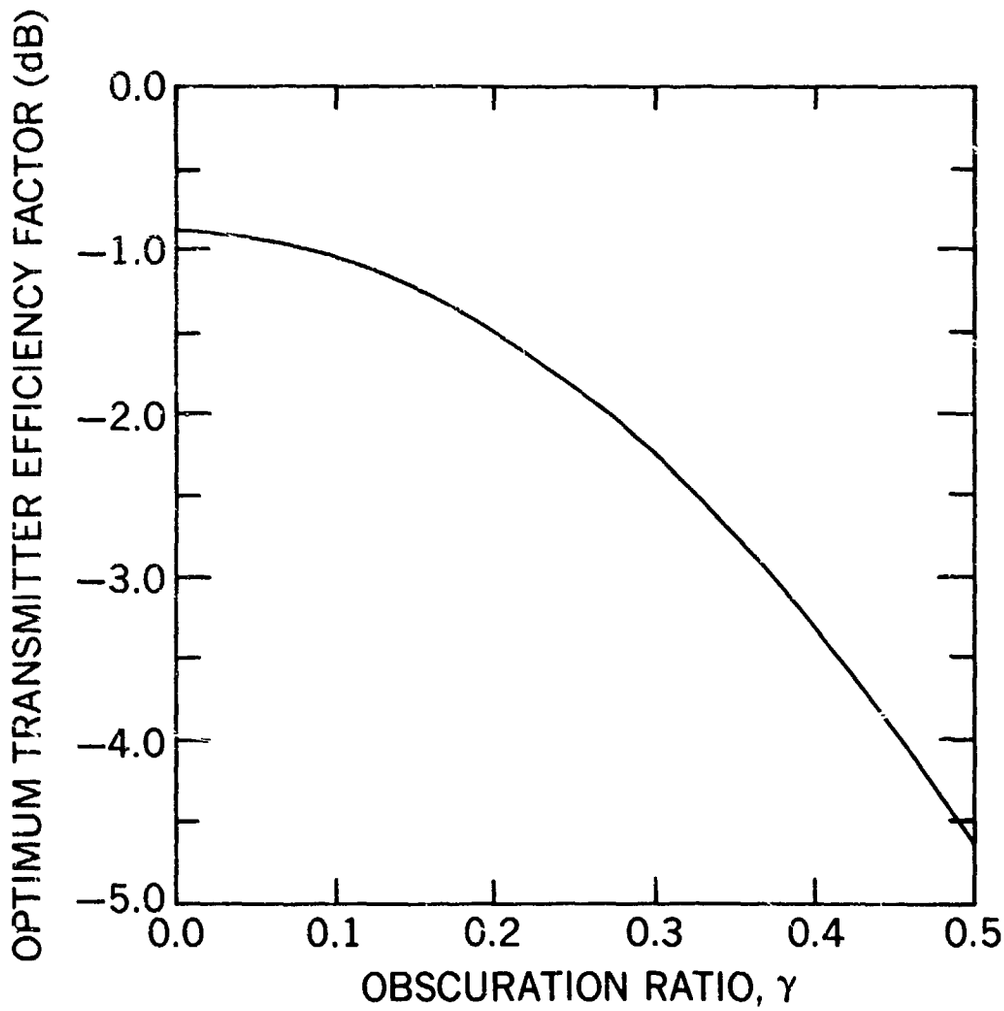

Figure 12. The axial gain of an optimum antenna relative to $4\pi A/\lambda^2$ as a function of obscuration ratio γ.

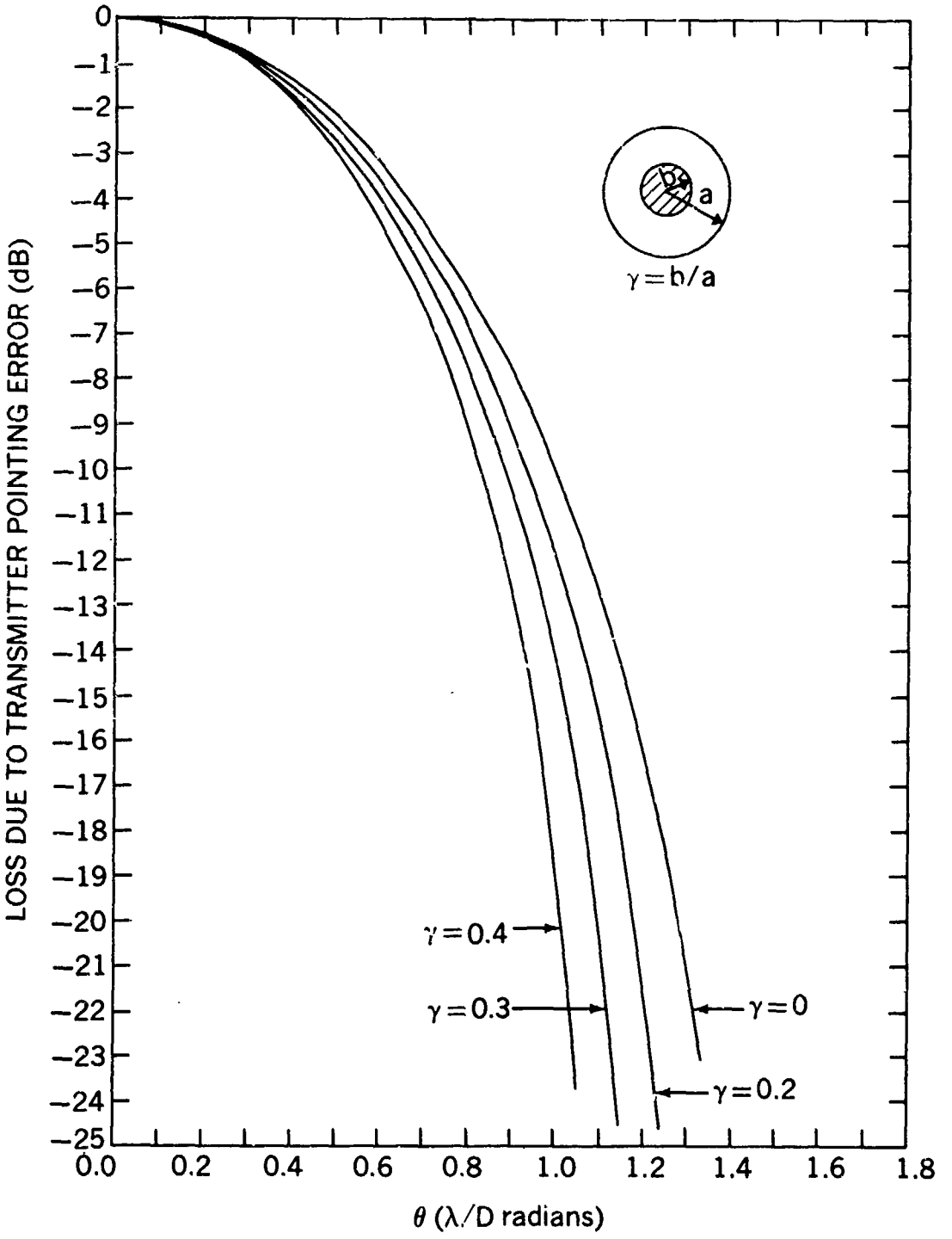

Figure 13. The dB loss due to transmitter pointing error as a function of the angular error θ for the optimum antenna configurations (maximum far-field gain) corresponding to four different obscuration ratios.

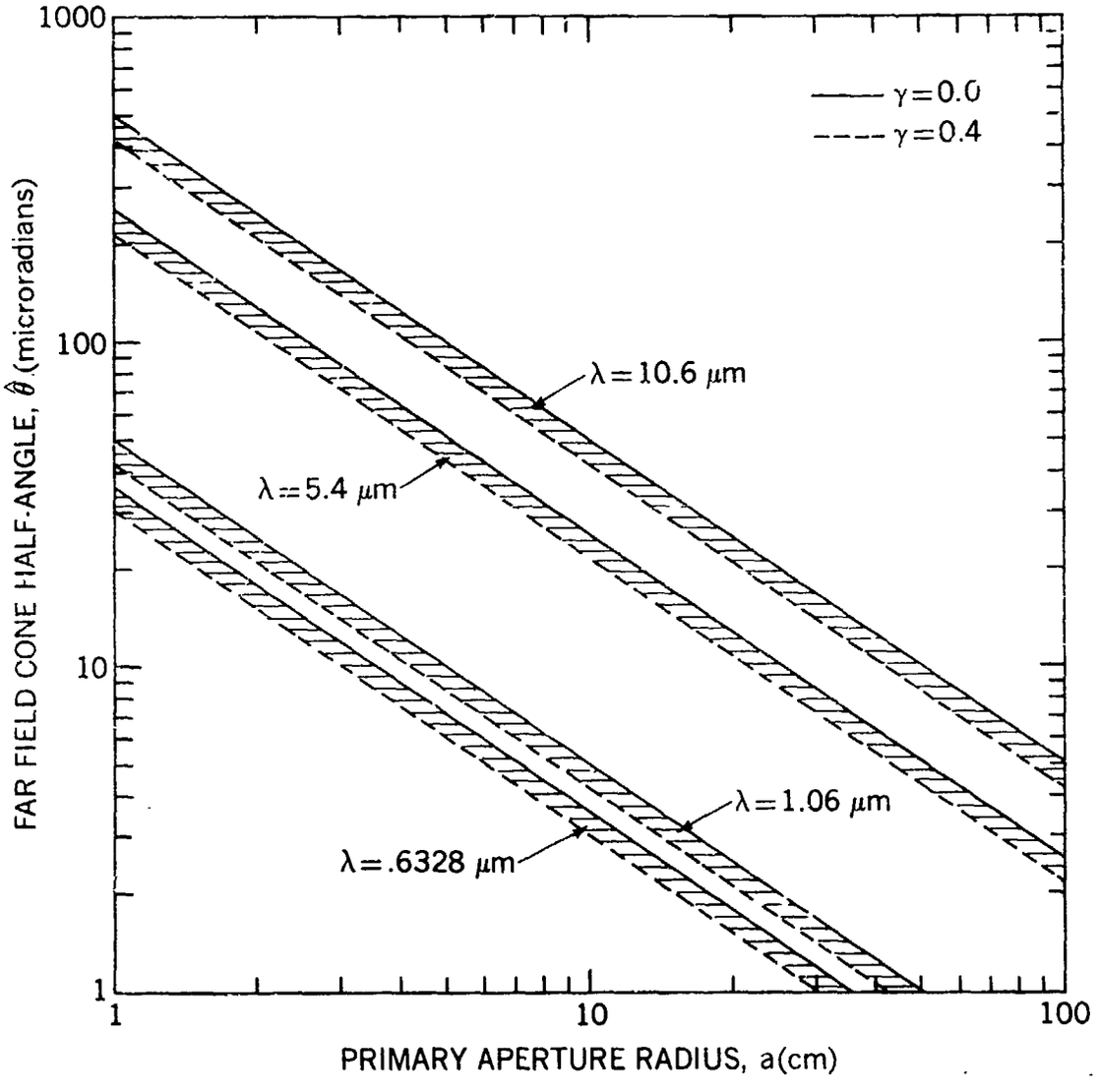

Figure 14. The half angle of the far-field transmitter cone produced by an antenna configuration optimized to give maximum on-axis gain as a function of the aperture radius a and wavelength λ. The half angle is defined as the angle from the optical axis to the $1/e^2$ intensity points.

Clearly, the total gain of an optimized antenna at any point in the far field can be obtained by simply summing the separate contributions from Figs. 11, 12, and 13, or from Figs. 6 through 11. The near field gain for optimized antennas is obtained by summing the contributions from Figs. 5 and 11 or by using Figs. 6 through 11 depending on whether the observation point is on or off the optical axis. The on-axis far field gains for arbitrary non-optimum antennas are calculated by summing the contributions from Figs. 4 and 11. For systems where the conventional definition of gain as described in Section 3.1 is more appropriate for analysis, an additional corrective factor is obtained from Fig. 3 and added to the total gain. The latter figure also gives the dB loss in total transmitted power due to the combined effects of truncation and central obscuration for arbitrary α and γ. The individual losses due to the aperture boundary and obscuration can be obtained by reading the truncation loss from the curve corresponding to $\gamma = 0$ in Fig. 3 and subtracting that value from the combined loss.

Figures 6 through 10 indicate that defocusing can indeed be used to spread the beam continuously over larger angles in the far field. Generally as the obscuration ratio increases, the gain profile tends to become more undulatory with angle. This lack of "smoothness" in the profile does not prevent the use of a defocused antenna in the acquisition of a target, however, since most acquisition techniques merely require the presence of a "star" on which to lock the tracking servos. For discrete jumps to cone angles an order of magnitude larger or more, one might consider transferring the laser beam to a much smaller parallel antenna or bypassing the antenna optics altogether and utilizing the natural divergence of the laser beam. The on-axis gain in dB of an untruncated laser beam is given by

$$G(db) = 10 \cdot \mathrm{Log}\left(\frac{8\pi^2\omega_0^2}{\lambda^2}\right) \tag{20}$$

where ω_0 is the radius of the laser beam waist as defined by Siegman[10] and is typically on the order of a few millimeters. Eq. (20) is plotted as a function of waist radius for several notable wavelengths in Fig. 15. The beam divergence in the far field for an untruncated laser beam is given by the expression[10]

$$\vartheta_\ell = \frac{\lambda}{\pi\omega_0} \tag{21}$$

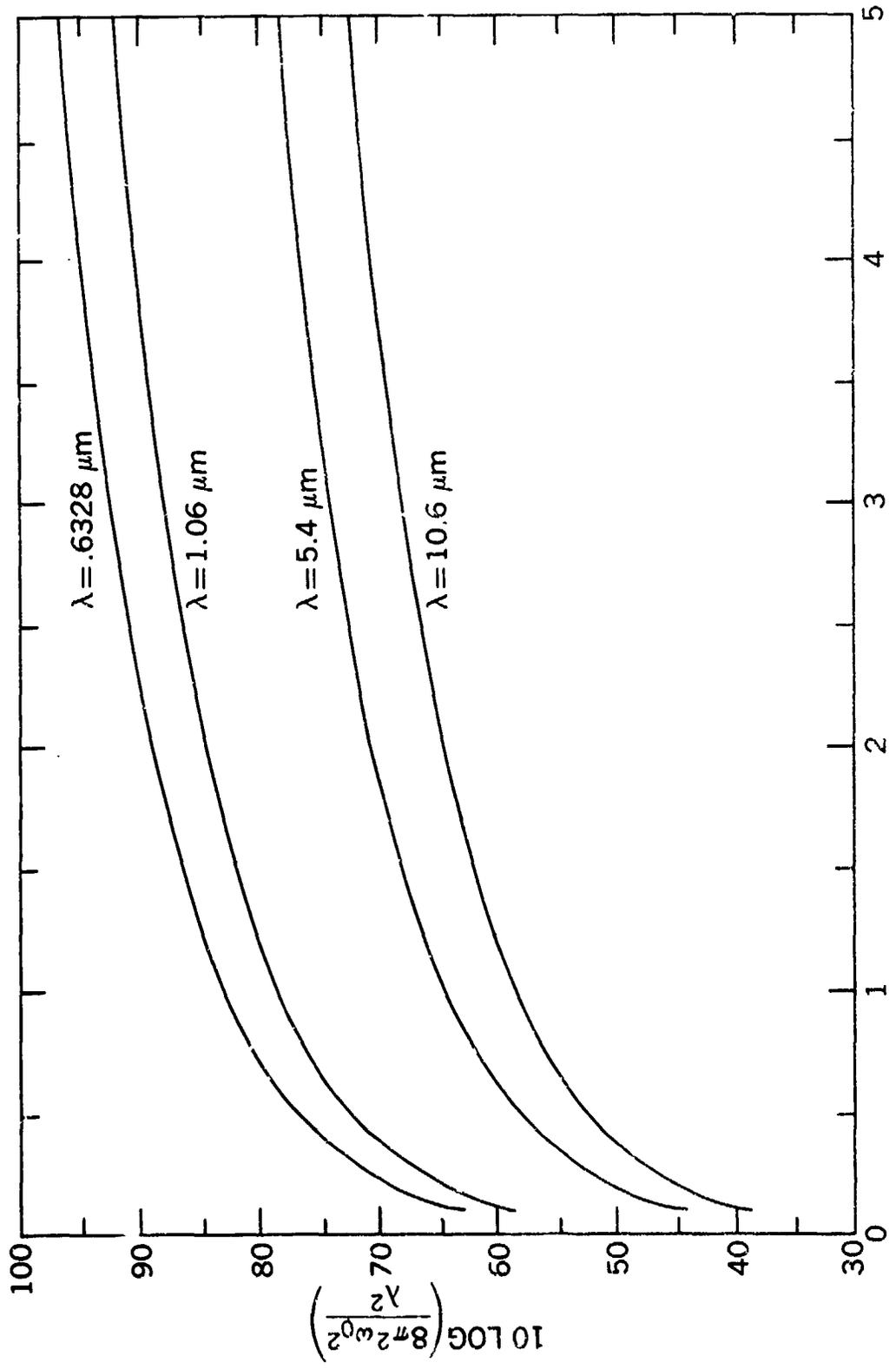

Figure 15. Far field on-axis gain in dB of an untruncated laser having a beam waist equal to ω_0 and a wavelength of operation λ

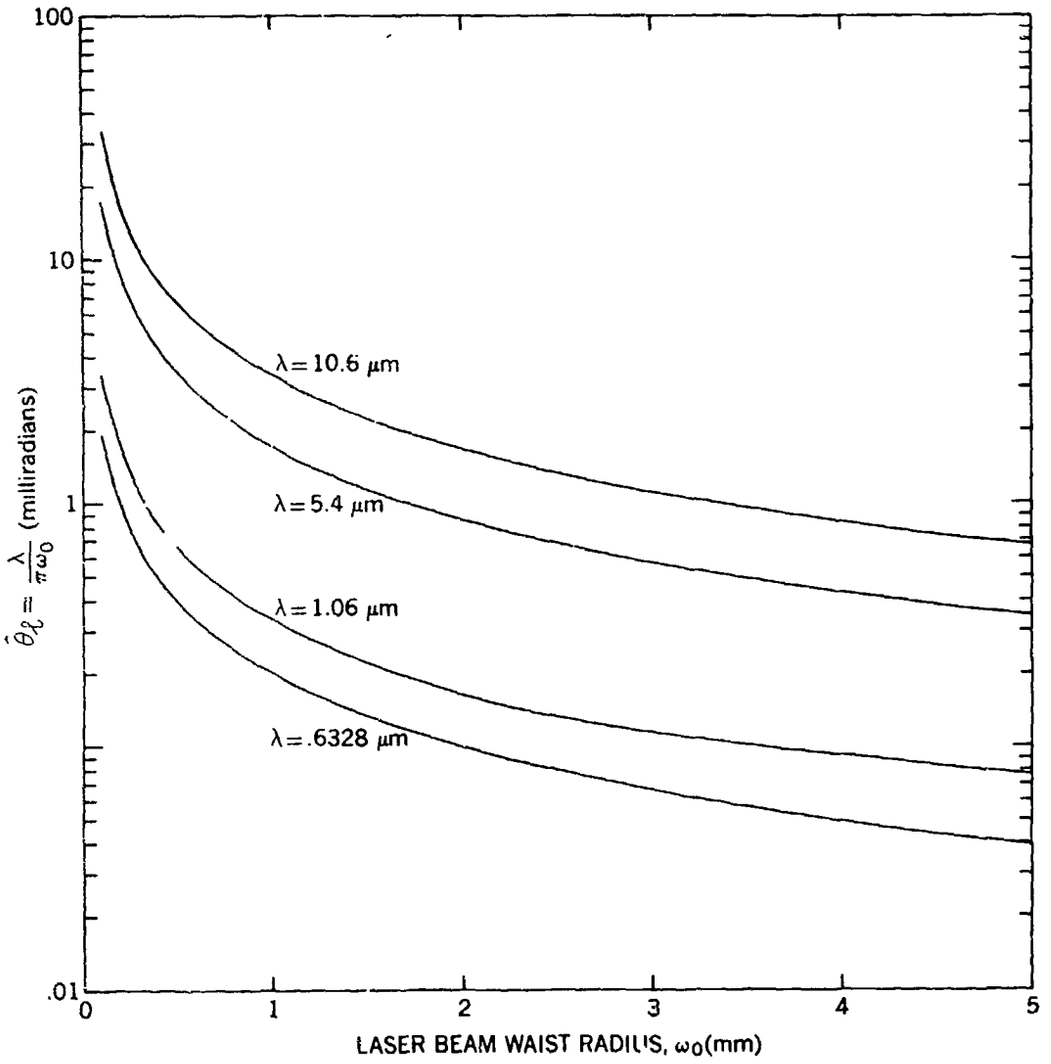

Figure 16. The half angle of the far field cone produced by an untruncated laser beam having a waist radius equal to ω_0 and a wavelength of operation λ. The half-angle is defined as the angle from the optical axis to the $1/e^2$ intensity points.

and is plotted in Fig. 16. The use of smaller parallel antennas or untruncated laser beams would result in much smoother gain profiles in the far field -- especially when compared to highly defocused ($\beta \approx 100$) obscured antennas which exhibit large excursions in the far field intensity of 10 dB and more near the optical axis as in Fig. 17(b). For systems operating on marginal signal to noise ratios, this would be equivalent to "blind" spots in the overall antenna pattern.

In concluding the transmitter discussion it is worthwhile to mention that a general computer program has been developed by R. F. Schmidt[14] which utilizes

vector diffraction theory and is capable of computing the effect of misalignment and secondary mirror supporting struts on the Fresnel and Fraunhofer patterns. The program has been used successfully in the evaluation of several microwave systems but would require modifications for application to optical and near infrared wavelength systems due principally to the integration algorithms used.

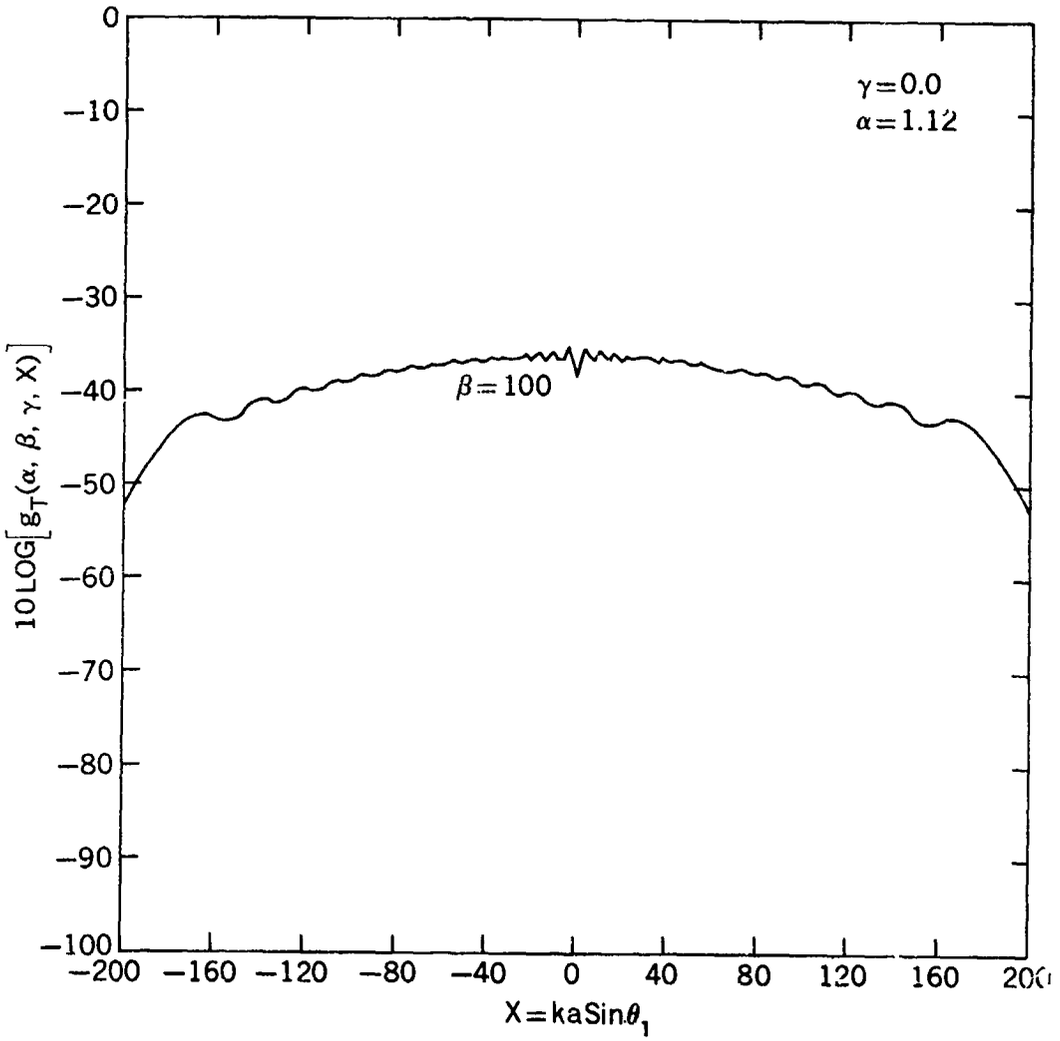

Figure 17a. Far field gain relative to $4\pi A/\lambda^2$ for a highly defocused antenna ($\beta = 100$) when the antenna is unobscured.

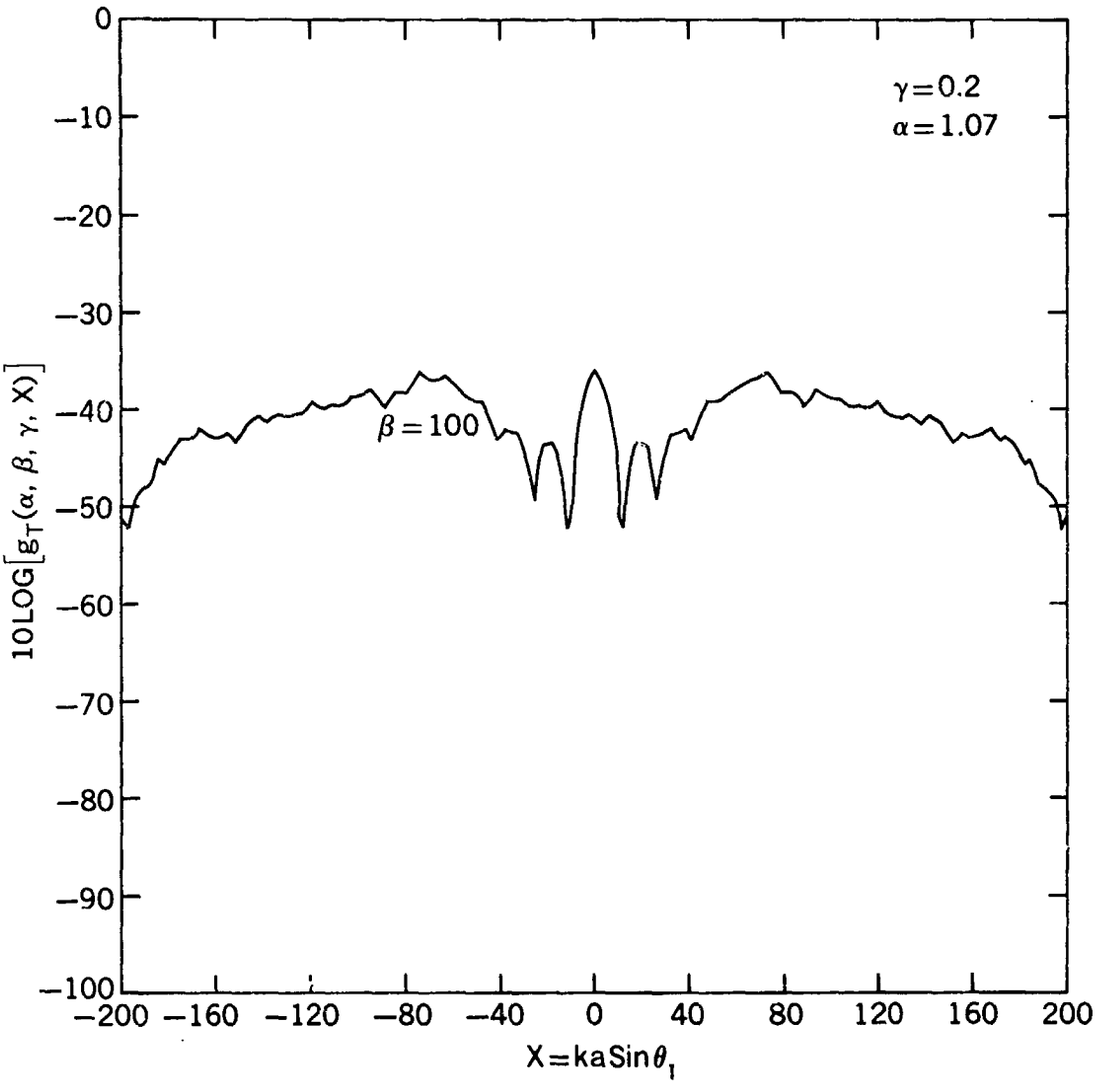

Figure 17b. Far field gain relative to $4\pi A/\lambda^2$ for a highly defocused antenna ($\beta = 100$) when the antenna has an obscuration ratio of 0.2.

3.5 An Illustrative Example

Consider a Cassegrainian optical antenna having a 10 cm exit aperture radius a, a 2 cm secondary mirror radius b, and illuminated by a laser operating in the Gaussian mode at 10.6 microns. The value of γ corresponding to this antenna is thus $\gamma = 0.2$. The far field case with plane waves incident on the antenna ($\beta = 0$) will be illustrated first, where we assume that the maximum on-axis gain from the antenna would be desirable. A value for α of 1.07 is obtained from Fig. 4 or by substitution of γ into Eq. (18). Maximum on-axis gain for the far field is found by adding the contributions from Fig. 11 and 12, from which we obtain 95.5dB and -1.5dB respectively. Referring back to Fig. 4 we can see how the maximum axial gain of 94 dB decreases with deviations in α from 1.07. Using Fig. 13 we can anticipate a 3 dB loss in gain for a $.55\lambda/D$ radians pointing error. At the 10.6 micrometer CO_2 wavelength this corresponds to a pointing error of 29 microradians. The full cone angle ($2\hat{\theta}$) of the beam in the far field is estimated to be 92 microradians by approximating the $\gamma = 0.2$ curve in Fig. 14.

If we were to defocus the antenna or move our observation point into the near field the value of β will no longer be zero and can be calculated using Eq. (10). Assuming $\beta' = \beta/2\pi = 1.46$, corresponding to one of the maxima in Fig. 5 for $\gamma = 0.2$, we obtain a transmitting efficiency factor of -13.9 dB. Adding the contribution from Fig. 11 yields a total on axis gain of 81.6 dB. The observation angle corresponding to the -3 dB point relative to the peak of the near field gain distribution is found from Fig. 8b to be ka Sin $\theta = 2.5$ yielding $\theta = 42$ microradians.

4.0 RECEIVER GAIN

4.1 Loss Due to the Central Obscuration

We now consider the gain of the previously described telescopes when used as receivers. We assume that the source of the radiation is sufficiently far away so that a uniform plane wave impinges on the receiving aperture. The gain of the receiver is defined as

$$G_R = \frac{4\pi A_R}{\lambda^2} = \frac{4\pi A}{\lambda^2}(1 - \gamma^2) \qquad (22)$$

where $A = \pi a^2$ is the area of the primary aperture as defined in Eq. (11). The quantity $(1 - \gamma^2)$ can be considered a receiver efficiency factor $g_R(\gamma)$ which takes into account the fraction of the impinging light scattered by the central obscuration. The receiver efficiency factor in dB is plotted in Fig. 18.

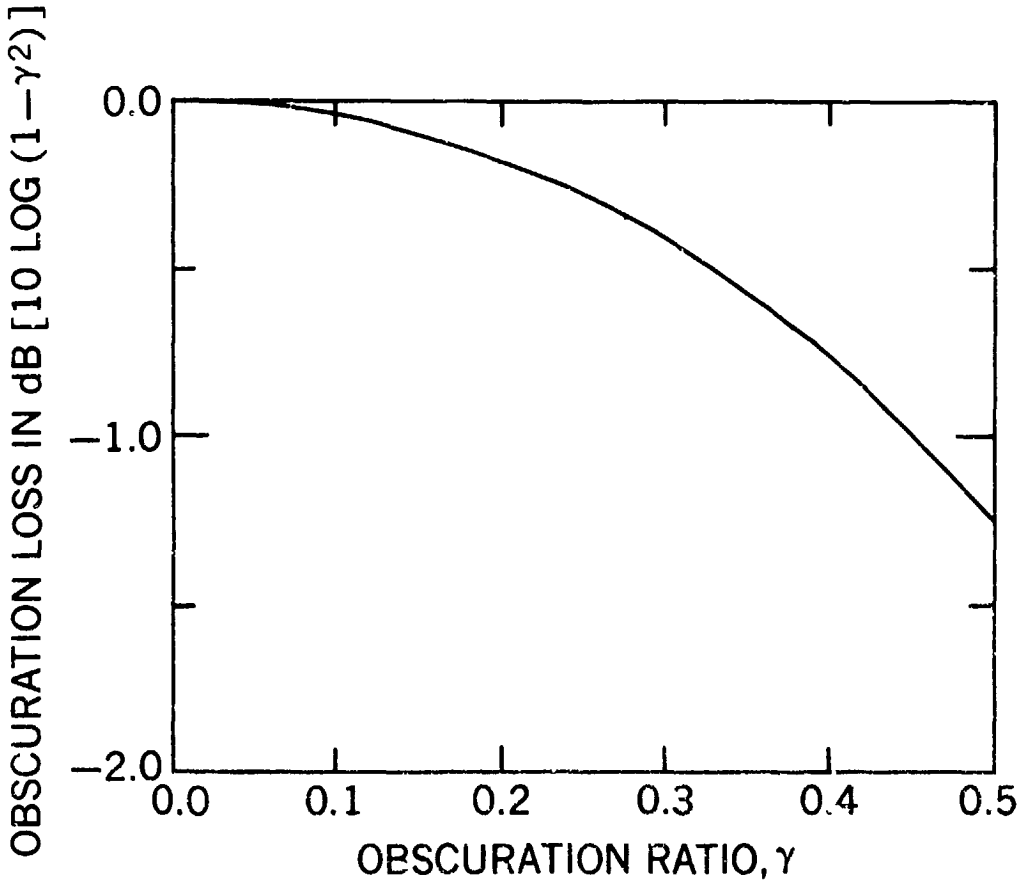

Figure 18. Receiver loss due to the central obscuration in dB.

4.2 Loss at the Detector

Although we have used the word "telescope" throughout the present article, the primary and secondary mirrors are actually equivalent to a large aperture lens of focal length f. The detector is placed in the back focal plane of this "lens" and the aperture plane containing the central obscuration lies a distance d (corresponding to the separation between the primary and secondary mirrors) in front of the "lens". Goodman[11] has shown that the electric field in the back focal plane is given by

$$E(x_f, y_f) = \frac{E_0 \exp\left[j \frac{k}{2f}\left(1 - \frac{d}{f}\right)(x_f^2 + y_f^2)\right]}{j\lambda f}$$

$$\cdot \int_{-\infty}^{\infty}\int_{-\infty}^{\infty} t_0(x_0, y_0) \exp\left[-j \frac{k}{f}(x_0 x_f + y_0 y_f)\right] dx_0\, dy_0 \tag{23}$$

where x_0 and y_0 and x_f and y_f are the Cartesian coordinates in the object plane and back focal plane respectively, E_0 is the amplitude of the uniform plane wave impinging on the aperture (object plane), and $t_0(x_0, y_0)$ is unity over unobscured portions of the aperture and zero over obscured areas. Converting to cylindrical coordinates and assuming centrally obscured apertures as before, we obtain

$$E(r_f, \phi_f) = \frac{E_0 \exp\left[j \frac{k}{2f}\left(1 - \frac{d}{f}\right) r_f^2\right]}{j\lambda f}$$

$$\cdot \int_b^a \int_0^{2\pi} \exp\left[-j \frac{k}{f} r_0 r_f \cos(\phi_0 - \phi_f)\right] r_0\, d\phi_0\, dr_0 \tag{24}$$

Since the "object" is circularly symmetric, the image in the focal plane is independent of ϕ_f and we can use arguments identical to those used in going from Eq. (3) to (4) to obtain

$$E(r_f) = -j \frac{E_0 k}{f} \exp\left[j \frac{k}{2f}\left(1 - \frac{d}{f}\right) r_f^2\right] \cdot \int_b^a J_0\left(\frac{k r_0 r_f}{f}\right) r_0\, dr_0$$

$$= -j \frac{E_0 a}{r_f} \exp\left[j \frac{k}{2f}\left(1 - \frac{d}{f}\right) r_f^2\right] \left[J_1\left(\frac{k a r_f}{f}\right) - \epsilon J_1\left(\frac{k a \epsilon r_f}{f}\right)\right] \tag{25}$$

where $\epsilon = b/a$ as before.

Equation (25) gives the distribution of electric field across the detector. We note from the exponential in Eq. (25) that if the entrance aperture of the telescope does not lie in the front focal plane of our equivalent "lens" then the phase front across the detector is not planar. Comparing Eq. (25) with the expressions in Appendix A indicates that the radius of curvature of the phase front is given by

$$C = \frac{f}{1 - \frac{d}{f}} \tag{26}$$

4.2.1 Direct Detection

In a direct detection system, the overall power into the detector is the important quantity. The fraction detected is simply given by

$$\eta_D = \frac{2\pi \int_0^{R_D} I(\rho_f)\, \rho_f\, d\rho_f}{2\pi \int_0^{\infty} I(\rho_f)\, \rho_f\, d\rho_f}$$

$$= \frac{2}{1-\gamma^2} \int_0^{R_D} \left[J_1\left(\frac{ka\rho_f}{f}\right) - \gamma J_1\left(\gamma \frac{ka\rho_f}{f}\right) \right]^2 \frac{d\rho_f}{\rho_f} \tag{27}$$

where R_D is the radius of the detector (assumed to be circular). By defining the variable $u = ka\rho_f/f$, the above equation simplifies to

$$\eta_D\left(\frac{kaR_D}{f}, \gamma\right) = \frac{2}{1-\gamma^2} \int_0^{\frac{kaR_D}{f}} [J_1(u) - \gamma J_1(\gamma u)]^2 \frac{du}{u} \tag{28}$$

where the fraction detected is a function of kaR_D/f and γ. The fractional power detected is plotted in dB in Fig. 19 against the parameter kaR_D/f for several values of γ.

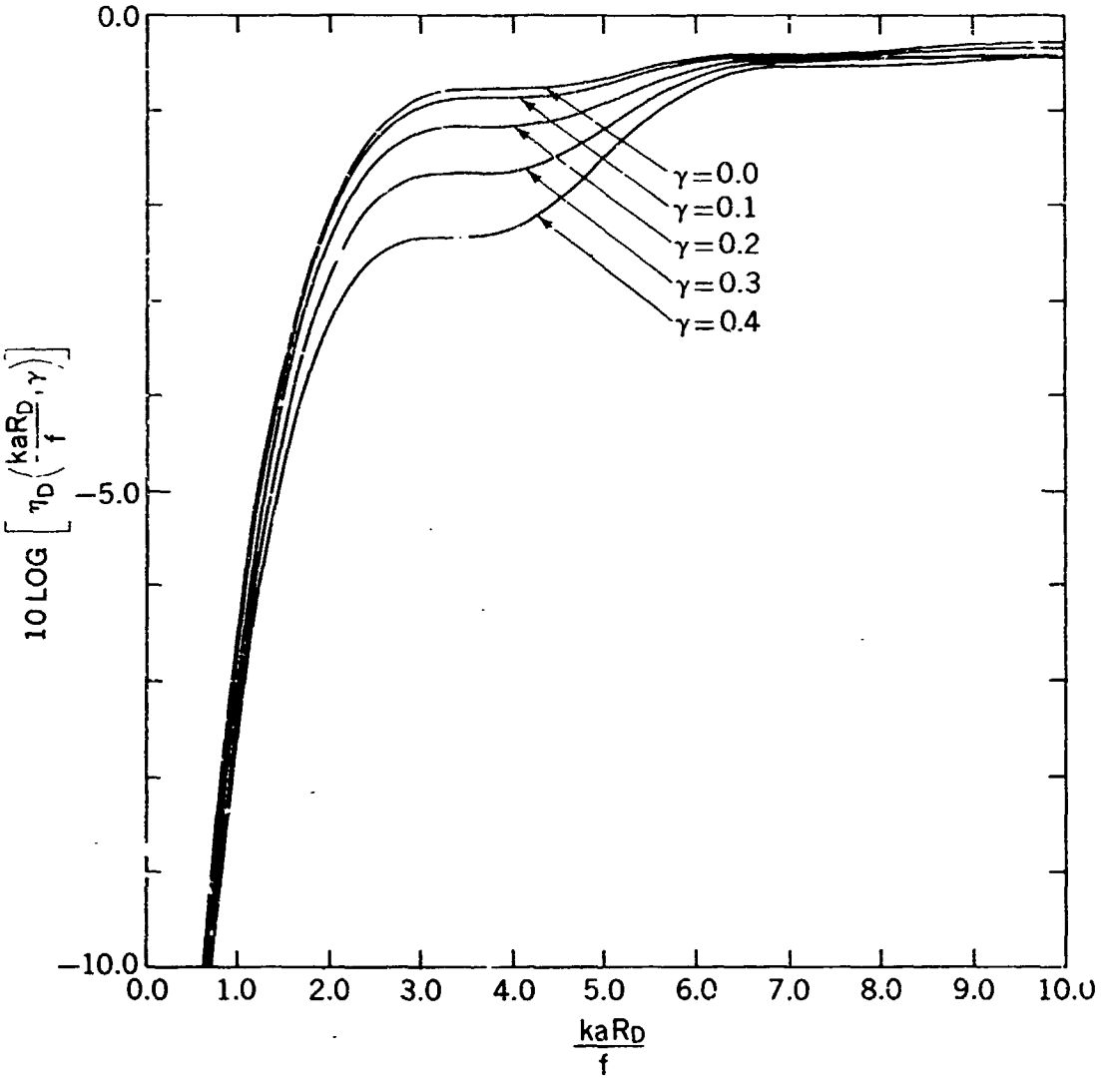

Figure 19. Fractional power detected as a function of the antenna obscuration ratio γ and the quantity ka R_D/f where $k = 2\pi/\lambda$, a is the aperture radius of the antenna, R_D is the detector radius and f is the focal length of the antenna. (Direct detection or "matched" heterodyne detection described in Section 4.2.2).

4.2.2 Heterodyne Detection

In a heterodyne detection system, the electric field is mixed with the local oscillator field which, for the moment,is assumed to be a uniform plane wave across the small aperture of the detector. The instantaneous power into the detector is given by

$$P(t) = 2\pi \int_0^{R_D} I(\rho_f)\, \rho_f\, d\rho_f$$

$$= 2\pi \int_0^{R_D} \left[\mathrm{Re}\left\{E(\rho_f)\, e^{j\omega_T t}\right\} + \mathrm{Re}\left\{E_{LO} e^{j(\omega_{LO} t - \phi)}\right\}\right]^2 \rho_f\, d\rho_f \qquad (29)$$

where E_{LO} is the real amplitude of the local oscillator field, ω_T and ω_{LO} are the transmitter and local oscillator frequencies, and ϕ is an arbitrary lag in the longitudinal phase of the two beams. Substituting Eq. (25) into (29) and ignoring components associated with frequencies of order $2\omega_T$ (which do not lie within the frequency response of the mixer), we obtain

$$P(t) = 2\pi \left\{ \frac{E_{LO}^2 R_D^2}{4} + \frac{E_{LO} E_0 f}{k} \left[\int_0^{\frac{ka R_D}{f}} \left[J_1(u) - \gamma J_1(\gamma u)\right] du \right] \sin\left[(\omega_T - \omega_{LO})\, t + \phi\right] \right\} \qquad (30)$$

where we have also ignored the relatively minor contribution of the transmitter power to the D.C. component and the curvature of the transmitter wavefront at the detector. The curvature can be ignored if

$$\left(1 - \frac{d}{f}\right) \frac{R_D^2}{\lambda f} << 1 \qquad (31)$$

which is often the case. Examination of the integral in Eq. (30) reveals that the detector radius R_{opt} which maximizes the signal at the intermediate frequency (IF) is determined by the first root of the equation

$$J_1\left(\frac{ka\, R_{opt}}{f}\right) - \gamma J_1\left(\gamma \frac{ka\, R_{opt}}{f}\right) = 0 \qquad (32)$$

which, as can be seen from Eq. (25), is also the determining equation for the nulls in the electric field distribution in the back focal plane of our equivalent lens. In other words, for optimum performance, the detector perimeter should

coincide with the first dark ring of the signal diffraction pattern. The use of a larger detector results in partial cancellation of the detected signal due to the change in sign of the electric field in spite of the fact that the detector captures more of the transmitter energy. The general solution to Eq. (32) was obtained numerically and is plotted as a function of γ in Fig. 20.

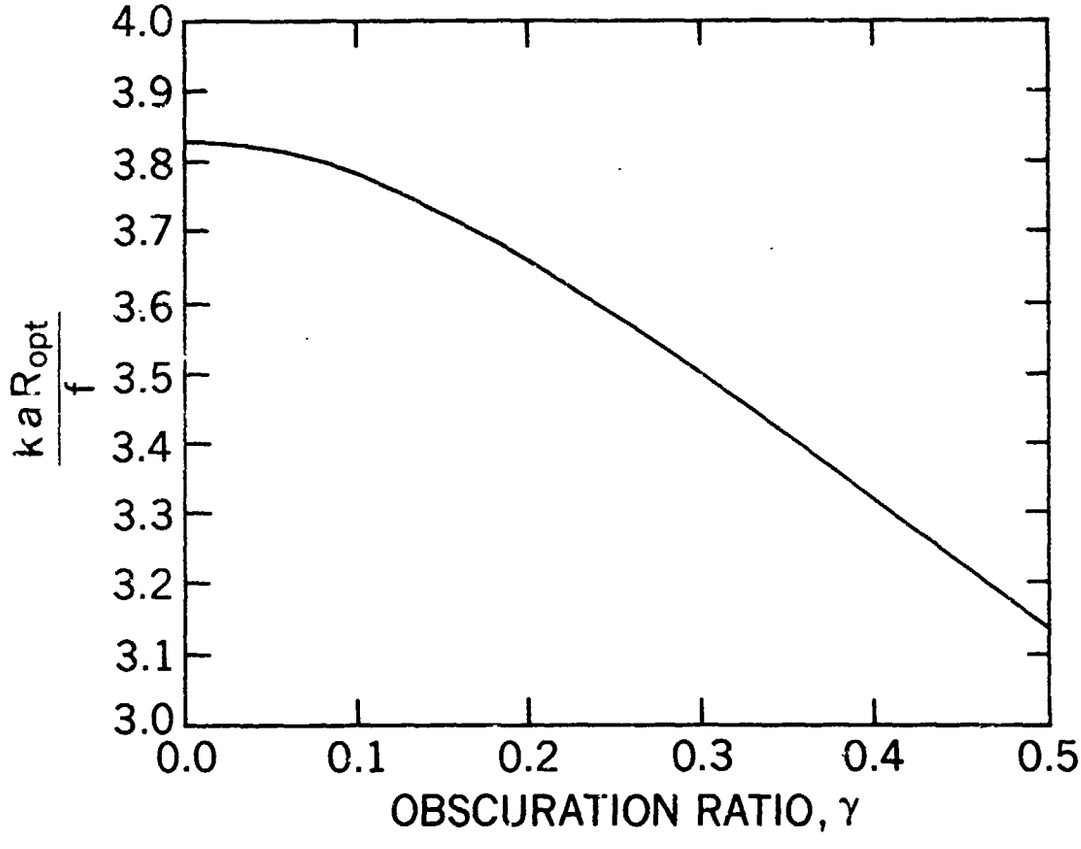

Figure 20. The introduction of a central obscuration into the aperture modifies the Airy pattern in the plane of the detector. This curve is used to match the antenna F-number (f/2a) to the detector radius (R_{opt}) so that the detector captures only the central disk of the signal diffraction pattern.

If we define $\overline{P}_R = E_0^2 \pi a^2 (1 - \gamma^2)/2$ as the time averaged power collected by the aperture and $\overline{P}_{LO} = E_{LO}^2 \pi R_{opt}^2/2$ as dc local oscillator power absorbed by the detector (uniform illumination only), then the mean square value of power in the IF component can be written

$$\overline{P_{IF}^2} = \frac{2\pi^2 E_{LO}^2 E_0^2 f^2}{k^2} \left[\int_0^{\frac{ka R_{opt}}{f}} [J_1(u) - \gamma J_1(\gamma u)]\, du\right]^2$$

$$= \frac{8 \overline{P}_R \overline{P}_{LO}}{(1-\gamma^2)} \left(\frac{ka R_{opt}}{f}\right)^{-2} \left[\int_0^{\frac{ka R_{opt}}{f}} [J_1(u) - \gamma J_1(\gamma u)]\, du\right]^2 \qquad (33)$$

The signal to noise ratio at the detector is defined as

$$\left(\frac{S}{N}\right) = \frac{\overline{i_s^2}}{\sum_n \overline{i_n^2}} \qquad (34)$$

where $\overline{i_s^2}$ is the mean square current generated in the detector due to the IF signal and $\overline{i_n^2}$ is the current generated by a particular noise process. The quantity $\overline{i_s^2}$ is in turn given by

$$\overline{i_s^2} = \left(\frac{e\tau G}{h\nu}\right)^2 \overline{P_{IF}^2} \qquad (35)$$

where e is the electronic charge, τ is the detector quantum efficiency, G is the detector gain (if any), h is Planck's constant, and ν is the photon frequency. In most references dealing with heterodyne detection, the mean square signal current is generally written in the form

$$\overline{i_s^2} = 2 \left(\frac{e\tau G}{h\nu}\right)^2 \overline{P}_{LO} \overline{P}_S \qquad (36)$$

Comparing Eqs. (33), (35), and (36), we infer

$$\bar{P}_S = \bar{P}_R \frac{4}{1-\gamma^2} \left(\frac{ka\,R_{opt}}{f}\right)^{-2} \left[\int_0^{\frac{kaR_{opt}}{f}} [J_1(u) - \gamma J_1(\gamma u)]\, du\right]^2 \tag{37}$$

Noting that the dimensionless parameter kaR_{opt}/f is a function of γ by virtue of Eq. (32), we can define $P_S = P_R\, \eta_H(\gamma)$ where

$$\eta_H(\gamma) = \frac{4}{1-\gamma^2} \left(\frac{ka\,R_{opt}}{f}\right)^{-2} \left[\int_0^{\frac{kaR_{opt}}{f}} [J_1(u) - \gamma J_1(\gamma u)]\, du\right]^2$$

$$= \frac{4}{1-\gamma^2} \left(\frac{ka\,R_{opt}}{f}\right)^{-2} \left[J_0\left(\gamma \frac{ka\,R_{opt}}{f}\right) - J_0\left(\frac{ka\,R_{opt}}{f}\right)\right]^2 \tag{38}$$

Thus, the time average power $\bar{P}_R$ actually received by the aperture must be multiplied by the factor $\eta_H(\gamma)$ to obtain the so-called "signal power" $\bar{P}_S$ which appears in the standard photodetector equations. The dB value of $\eta_H(\gamma)$ for uniform illumination is plotted versus γ in Fig. 21(b). The above calculations were performed under the assumption that the local oscillator beam illuminates the detector uniformly. The efficiency of the receiver can be improved, however, by focusing the local oscillator energy onto the detector. The most general system one can imagine is one in which the local oscillator beam is focused by a separate set of optics into the detector. If we allow the effective F numbers of the signal and local oscillator optics to be given by F_S and F_{LO} and the respective central obscurations to be given by γ_S and γ_{LO}, we obtain the general result

$$\eta_H\left(\frac{ka\,R_D}{f}, \gamma_S, \gamma_{LO}, \frac{F_S}{F_{LO}}\right)$$

$$= \frac{2}{1-\gamma_S^2} \frac{\left[\int_0^{\frac{kaR_D}{f}} \left[J_1\left(\frac{F_S}{F_{LO}} u\right) - \gamma_{LO} J_1\left(\gamma_{LO} \frac{F_S}{F_{LO}} u\right)\right]\left[J_1(u) - \gamma_S J_1(\gamma_S u)\right] \frac{du}{u}\right]^2}{\int_0^{\frac{kaR_D}{f}\left(\frac{F_S}{F_{LO}}\right)} [J_1(u) - \gamma_{LO} J_1(\gamma_{LO} u)]^2 \frac{du}{u}} \tag{39}$$

The latter equation is obtained by substituting two electric field distributions of the form given by Eq. (25) into Eq. (29) and proceeding with the calculations as in the uniformly illuminated case.

A system of practical interest is one in which the detector captures only the central lobe of the signal Airy disk but the local oscillator beam is partially focused onto the detector by an unobscured lens ($\gamma_{LO} = 0$). Eq. (39) then reduces to

$$\eta_H \left(\frac{kaR_{opt}}{f}, \gamma, 0, \frac{F_S}{F_{LO}} \right) = \frac{2}{1-\gamma^2} \frac{\left[\int_0^{\frac{kaR_{opt}}{f}} J_1 \left(\frac{F_S}{F_{LO}} u \right) \left[J_1(u) - \gamma J_1(\gamma u) \right] \frac{du}{u} \right]^2}{\int_0^{\frac{kaR_{opt}}{f} \left(\frac{F_S}{F_{LO}} \right)} J_1^2(u) \frac{du}{u}} \quad (40)$$

where kaR_{opt}/f is defined as before and has been plotted against γ in Fig. 20. Eq. (40) is plotted versus the parameter F_S/F_{LO} in Fig. 21(a) for several values of γ. The limiting value of η_H as $F_S/F_{LO} \rightarrow 0$ in the latter figure corresponds to unfocused uniform illumination by the LO. The comparison of these limiting values with the uniform illumination curve in Fig. 21(b) calculated using Eq. (38) at the points $\gamma = 0.0, 0.1, 0.2, 0.3$ and 0.4 verifies this relationship. As the LO beam is focused, the receiver efficiency increases until the first dark rings of the local oscillator and signal diffraction patterns coincide. Focusing the LO beam still further causes the first outer intensity ring of the diffraction pattern to fall on the detector resulting in a partial cancellation of the signal at the intermediate frequency and reducing the overall efficiency of the receiver.

The ratio of the F numbers which results in maximum efficiency for a heterodyne receiver is given by

$$\left(\frac{F_S}{F_{LO}} \right)_{opt} = 3.83 \left(\frac{kaR_{opt}}{f} \right)^{-1} \quad (41)$$

where kaR_{opt}/f is a function of the obscuration ratio γ and is plotted in Fig. 20. The overlap integral of the two electric field distributions is maximized when the above condition holds and thus the signal at the intermediate frequency is strongest.

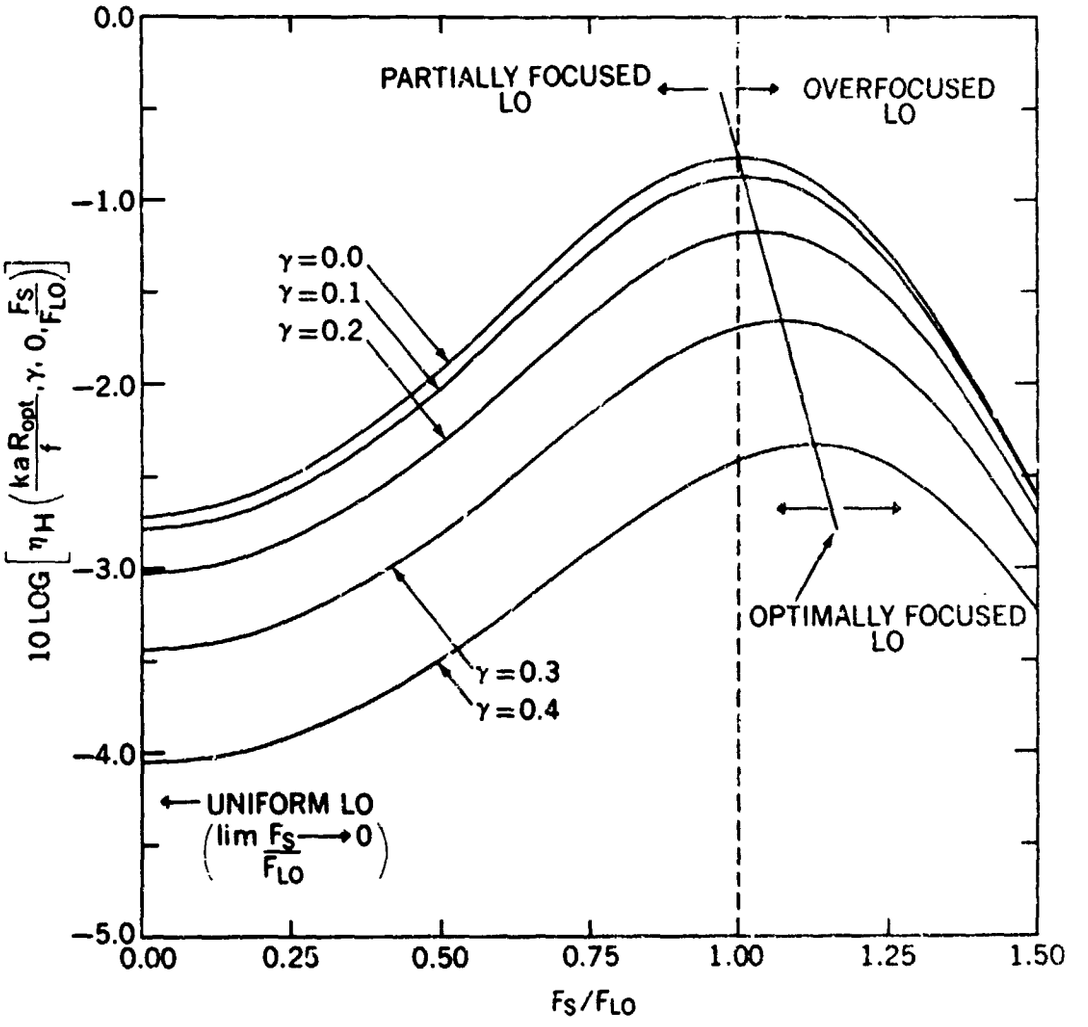

Figure 21a. The heterodyne detection loss in dB as a function of F_S/F_{LO} where F_S is the F-number of the optical antenna and F_{LO} is the F-number of the local oscillator focusing optics. The limiting values as $F_S/F_{LO} \rightarrow 0$ give the detection efficiency for uniform illumination by the local oscillator. The efficiency improves as the local oscillator is focused more effectively on the detector until the second bright ring of the LO diffraction pattern begins to fall on the detector. This results in partial cancellation of the IF signal and reduces the detection efficiency.

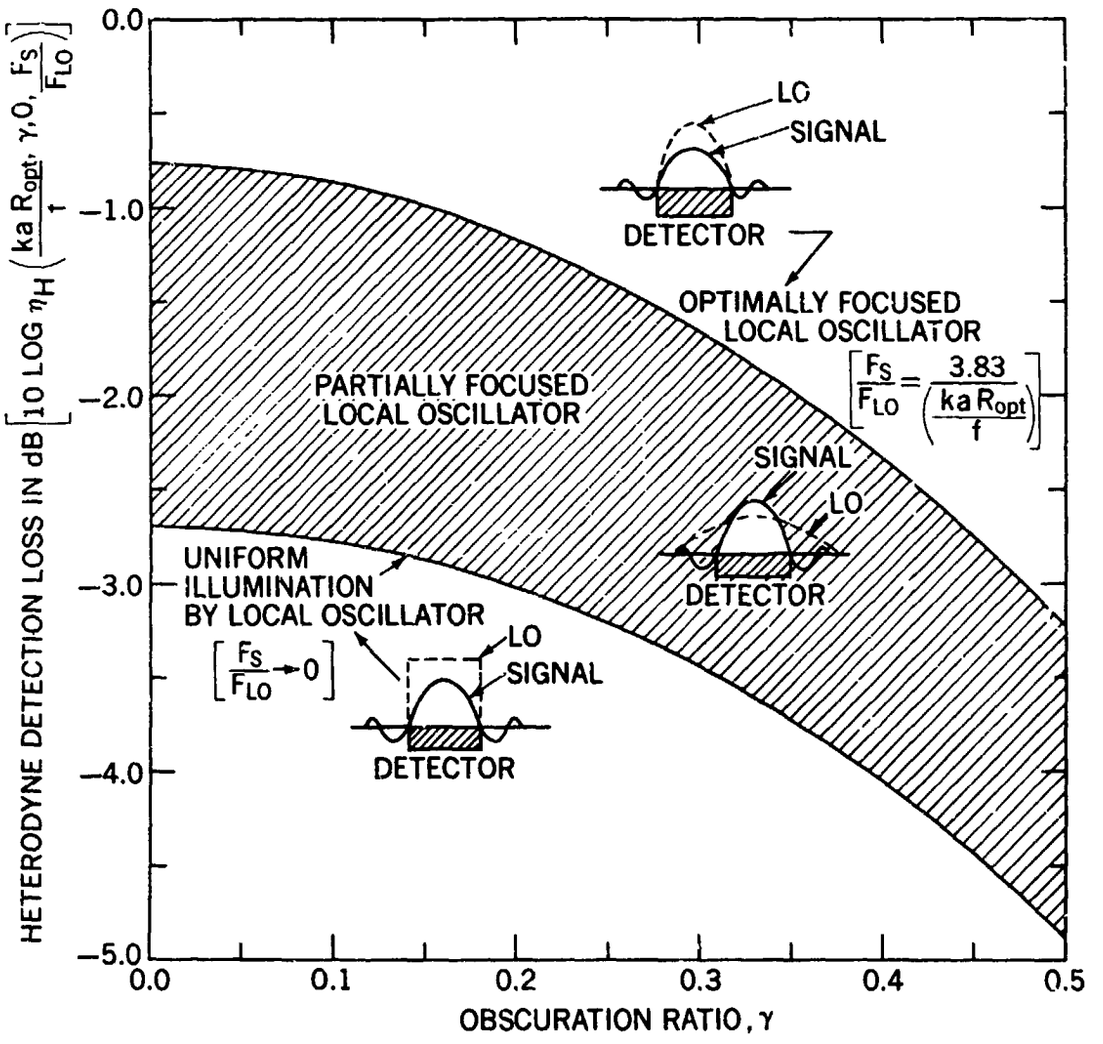

Figure 21b. The heterodyne detection loss in dB as a function of obscuration ratio γ. The lower boundary of the shaded region is the detection efficiency for uniform illumination by the LO. The upper boundary is the optimum detection efficiency obtained when the first dark rings of the signal and LO diffraction patterns coincide with the perimeter of the circular detector. This upper boundary corresponds to the peaks in Fig. 20(a). The shaded region designates the intermediate range of efficiencies obtainable with partially focused local oscillator beams.

Of course, in deriving Eq. (38), we have assumed that the total DC local oscillator power into the detector (and hence the detector shot noise) is held constant. The increase in receiver efficiency brought about by focusing the LO occurs because we have concentrated a greater fraction of the total LO power near the center of the detector where the signal intensity is strongest thereby maximizing the overlap integral. Upon substitution of Eq. (41) into (40) we obtain

$$\eta_H\left[\frac{ka R_{opt}}{f},\ \gamma,\ 0,\ 3.83\left(\frac{ka R_{opt}}{f}\right)^{-1}\right]$$

$$= \frac{2}{1-\gamma^2}\ \frac{\left[\int_0^{\frac{ka R_{opt}}{f}} J_1\left[3.83\left(\frac{ka R_{opt}}{f}\right)^{-1} u\right]\left[J_1(u) - \gamma J_1(\gamma u)\right]\frac{du}{u}\right]^2}{\int_0^{3.83} J_1^2(u)\,\frac{du}{u}} \qquad (42)$$

Again, since $ka R_{opt}/f$ is uniquely defined for each value of γ, the latter expression can be plotted versus the single parameter γ to yield the upper curve in Fig. 21(b) labeled "Optimally Focused Local Oscillator". The latter curve represents a lower limit on the detector loss under the assumption that the detector captures only the central lobe of the signal distribution. The losses for partially focused local oscillator beams (the full central disk of the LO pattern does not fall on the detector) fall in the shaded region between the two curves.

We now consider one final very special case where the F number of the local oscillator beam matches the F number of the signal beam ($F_s/F_{LO} = 1$) and a mask is constructed over the focusing lens for the local oscillator such that $\gamma_{LO} = \gamma_S = \gamma$. We obtain from Eq. (39)

$$\eta_H\left(\frac{ka R_D}{f},\ \gamma,\ \gamma,\ 1\right) = \frac{2}{1-\gamma^2}\left[\int_0^{ka R_D/f}\left[J_1(u) - \gamma J_1(\gamma u)\right]^2\frac{du}{u}\right] \qquad (43)$$

Under the latter conditions, the electric field distributions of the two beams are identical in the plane of the detector except for a constant amplitude factor. The resulting equation for the efficiency is identical to Eq. (28) obtained for direct detection which was plotted previously in Fig. 19. Unlike the

situations discussed previously, the detector dimensions can be enlarged beyond the central lobe in the signal diffraction pattern without encountering field cancellation effects.

4.3 Receiver Summary

Figure 11 gives the dB gain of an unobscured antenna of radius a for a wavelength λ. Figure 18 gives the dB loss in received power due to blockage of the incoming light by the central obscuration. Figures 19 and 21 give the dB loss at the detector for direct detection and heterodyne detection respectively.

For a direct detection system, the total receiver gain can be obtained by summing the separate contributions from Figs. 11, 18 and 19. Of course, the effect of lossy optical elements or non-unity detector gains and quantum efficiencies must be separately accounted for.

In heterodyne (or homodyne) detection systems, the effective receiver gain depends on the electric field distributions of the local oscillator and signal beams across the detector. Good performance is obtained when the first dark rings surrounding the central Airy disks of the focused signal and LO diffraction patterns coincide with the detector perimeter. The system experiences significant degradation when the LO uniformly illuminates the detector or is only partially focused on the detector. Large obscuration ratios degrade the receiver gain for two reasons: (1) greater blockage of the incoming radiation results; and (2) a smaller fraction of the total received energy is contained within the central lobe. The total receiver gain is obtained by summing the separate contributions from Figs. 11, 18 and 21. The optimum ratio of detector size to antenna F number can be inferred from Fig. 20. The efficiency of a heterodyne detection system can be further improved by constructing an appropriate mask over the lens which focuses the local oscillator beam onto the detector. If the obscuration ratio of the mask matches the value of the obscuration ratio for the antenna and if the F numbers of the signal and LO optics are the same, then the field distributions of the two beams across the face of the detector are identical except for a constant amplitude factor. As a result, the detector size can be enlarged to contain the outer rings of the diffraction distributions without encountering field cancellation effects. In this very special case, the losses are identical to those suffered in a direct detection scheme and the total receiver gain is calculated using Figs. 11, 18 and 19. Systems in which the local oscillator is focused onto the detector require more stringent alignment tolerances [12], however, and care must be taken to insure that the phase fronts of the two beams do not vary widely over the detector dimensions. Calculations of the power distributions in the near field and in the vicinity of the focus for Gaussian beams focused through annular apertures have been carried out by Holmes et al.[13] The present work assumes that the LO spot size is large compared to the effective aperture of the focusing lens.

4.4 An Illustrative Example

We consider a Cassegrainian telescope with a 20-cm diameter primary and a 4-cm secondary mirror. Thus, we have a = 10 cm and $\gamma = 0.2$. From Fig. 11, we obtain a value of 95.5 dB at a wavelength of 10.6 microns. This represents the theoretical upper limit on the gain available from an unobscured antenna having a diameter of 20 cm. Fig. 18 indicates that 0.2 dB is lost due to blockage of the incoming radiation by the secondary mirror. If the local oscillator illuminates the detector uniformly, an additional loss of -3 dB is evident from Fig. 21(b) yielding a total receiver gain of 92.3 dB. Focusing the LO so that the two central disks are barely contained within the detector raises the receiver gain to 94.1 dB. The appropriate ratio of detector radius to antenna focal length can be obtained using the relation $ka\, R_{opt}/f = 3.67$ from Fig. 20.

ACKNOWLEDGMENT

The authors wish to express their appreciation to J. H. McElroy and P. O. Minott for helpful discussions and to G. Schiffner who laid some of the ground work for the article while he held a National Research Council Post-doctoral Fellowship at the Goddard Space Flight Center.

REFERENCES

1. J. P. Campbell and L. G. DeShazer, "Near Fields of Truncated-Gaussian Apertures," Journal of the Optical Society of America, Vol. 59, No. 11, (November 1969), pp. 1427-1429.

2. A. L. Buck, "The Radiation Pattern of a Truncated Gaussian Aperture Distribution," Proceedings of the IEEE, Vol. 55, No. 3, (March 1967), pp. 448-450.

3. J. A. Kauffman, "The Calculated Radiation Patterns of a Truncated Gaussian Aperture Distribution," IEEE Trans. on Antennas and Propagation, Vol. AP, No. 13, (May 1965), pp. 473-474.

4. J. W. Goodman, Intro to Fourier Optics, (McGraw-Hill Book Company, New York, N.Y., 1964) p. 60.

5. J. Mathews and R. L. Walker, Mathematical Methods of Physics, (W. A. Benjamin, Inc., New York, N.Y., 1964), p. 177.

6. W. N. Peters and A. M. Ledger, "Techniques for Matching Laser TEM Mode to Obscured Circular Apertures," Applied Optics, Vol. 9, No. 6, (June 1970), pp. 1435-1442.

7. C. McIntyre, W. N. Peters, C. Chi, and H. F. Wischnia, "Optical Components and Technology in Laser Space Communications Systems," Proceedings of the IEEE, Vol. 58, No. 10, (October 1970), pp. 1491-1503.

8. Intensity is defined here as the square of the amplitude of the electric field where some constant factors have been ignored. The term "irradiance" has also been used in this instance.

9. S. Silver, Microwave Antenna Theory and Design, (McGraw-Hill Book Company, New York, N. Y., 1949), p. 177.

10. A. E. Siegman, An Introduction to Lasers and Masers, Chapter 8, (McGraw-Hill Book Company, New York, N. Y., 1971).

11. Goodman, op. cit., p. 86.

12. B. J. Peyton, A. J. DiNardo, G. M. Kanischak, F. R. Arams, R. A. Lange, and E. W. Sard, "High-Sensitivity Receiver for Infrared Laser Communications", IEEE J. Quant. Electr., QE-8, No. 2, (February 1972), pp 252-263.

13. D. A. Holmes, J. E. Korka, and P. V. Avizonis, "Parametric Study of Apertured Focused Gaussian Beams", Applied Optics, Vol. 11, No. 3, (March 1972), pp 565-574.

14. R. F. Schmidt, "The Calculation of Electromagnetic Fields in the Fresnel and Fraunhofer Regions Using Numerical Integration Methods", NASA/GSFC X-811-71-392, July 1971.

APPENDIX A

MATHEMATICAL REPRESENTATION OF SPHERICAL WAVEFRONTS AT AN APERTURE

Consider a spherical wave emanating from a point source a distance R from a diffracting aperture as in Fig. A. Consider also a Gaussian amplitude function superimposed on the wavefront. The electric field at the aperture can then be expressed as

$$E_0(r_0) = E e^{jkr} e^{-r_0^2/\omega^2}$$

Assuming the curvature of the phase front is much larger than the aperture allows us to write the approximation

$$r = (R^2 + r_0^2)^{1/2} = R\left(1 + \frac{r_0^2}{R^2}\right)^{1/2} \simeq R\left[1 + \frac{r_0^2}{2R^2}\right].$$

The field can now be approximated by

$$E_0(r_0) = E e^{jkR} e^{jkr_0^2/2R} e^{-r_0^2/\omega^2}$$

where e^{jkR} is a constant phase factor that is lost in a calculation of the intensity at a point beyond the aperture.

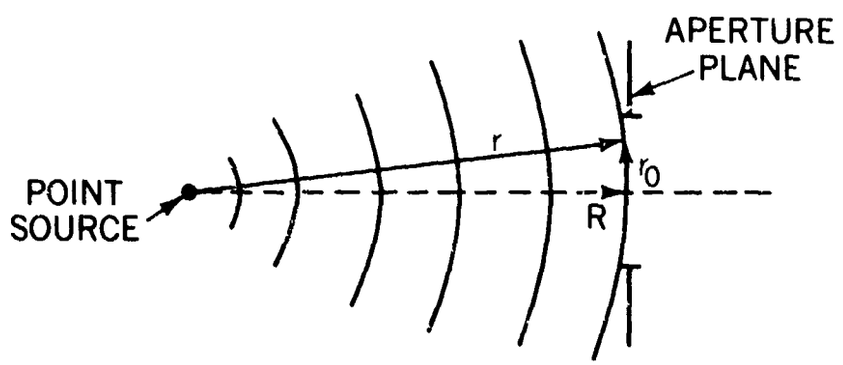

Figure A1. Mathematical representation of curved wavefronts at an aperture.

APPENDIX B

SECOND ORDER PERTURBATION ANALYSIS OF OBSCURED APERTURES

We are interested in obtaining an approximate analytical solution to the transcendental equation

$$\frac{2\alpha^2 + 1}{2\alpha^2\gamma^2 + 1} e^{-\alpha^2(1-\gamma^2)} = 1. \tag{17}$$

In Section 4, we obtained the solution $\alpha_0 = 1.12$ for the special case $\gamma = 0$. We will assume that an approximate solution of the form

$$\alpha \approx \alpha_0 + \delta\alpha_1 + \delta^2\alpha_2$$

can be obtained where α_1 and α_2 are the first and second order corrections to the zeroth order solution α_0 for small γ, and δ is a dimensionless parameter which simply monitors the relative magnitudes of the individual terms. Since γ^2 is the perturbing quantity in equation (17), we associate a factor of δ with each factor of γ^2. Ignoring terms of order δ^3 or higher allows us to rewrite (17) (after much algebra) as

$$(2\alpha_0^2 + 1) + \delta(4\alpha_0\alpha_1) + \delta^2(4\alpha_0\alpha_2 + 2\alpha_1^2)$$

$$= e^{\alpha_0^2} \left\{ 1 + \delta(\alpha_0^2\gamma^2 + 2\alpha_0\alpha_1) \right.$$

$$\left. + \delta^2 \left[2\alpha_0\alpha_1\gamma^2 + 2\alpha_0\alpha_2 + \alpha_1^2 + \frac{(2\alpha_0\alpha_1 - \alpha_0^2\gamma^2)^2}{2} + 2\alpha_0^2\gamma^2(2\alpha_0\alpha_1 - \alpha_0^2\gamma^2) \right] \right\}$$

Collecting terms of zero order in δ gives

$$(2\alpha_0^2 + 1) e^{-\alpha_0^2} = 1$$

which is the defining equation for α_0 with the solution $\alpha_0 = 1.12$.

Collecting terms of first order in δ and solving for a_1 gives

$$a_1 = \frac{a_0 e^{a_0^2}}{2(2 - e^{a_0^2})} \gamma^2 = -1.30\,\gamma^2.$$

The terms of second order in δ result in an equation for a_2, that is

$$a_2 = \frac{1}{2a_0(2 - e^{a_0^2})} \left\{ \frac{e^{a_0^2}}{2} [4a_0a_1\gamma^2 + 2a_1^2 + 4a_0^2a_1^2 + 4a_0^3a_1\gamma^2 - 3a_0^4\gamma^4] - 2a_1^2 \right\}$$

$$= 2.12\,\gamma^4.$$

Thus, to second order the optimum aperture to beamwidth ratio for maximum axial gain for an arbitrary obscuration ratio is given by

$$a \approx a_0 + a_1 + a_2 = 1.12 - 1.30\,\gamma^2 + 2.12\,\gamma^4. \tag{18}$$

Comparisons of the above approximation to exact solutions of equation (13) obtained on a computer for several test values of γ indicate an accuracy to within $\pm 1\%$ for $\gamma \leq 0.4$.

APPENDIX C

PROGRAM P – GAIN

The program, which has been named P-Gain, for power gain, is written in Fortran IV in the complex double-precision mode and computes near and far field antenna gain patterns. Eq. (12),

$$g_T(\alpha, \beta, \gamma, \chi) = 2\alpha^2 \left| \int_{\gamma^2}^{1} e^{i\beta u}\, e^{-\alpha^2 u}\, J_0(X \sqrt{u})\, du \right|^2 \qquad (12)$$

reproduced here from Section 3.1, is the basis for the calculation. The program owes its bulk, somewhat, to the injection of a large number of auxiliary comments and to the rather sophisticated plotting technique (Wolfplot) employed.

Care is taken to insure accuracy while attempting to incorporate speed into the computation. The integration is performed by a slightly modified version of a double precision 12-point Gaussian quadrature subroutine. The routine was revised to allow complex integration thereby reducing the computation time of the program by approximately one-half.

The separation of the annular region of the antenna aperture into integrable divisions to obtain sufficient accuracy was determined by analyzing the integrand. Location of the observation point, i.e. its perpendicular distance to the optical axis in the near or far field, dictates whether the Bessel function or the complex exponential function has the higher frequency of oscillation. The number of half cycles of the faster oscillating function prescribes the number of regions of integration in the program. The integration limits for each quadrature integration are then taken over each half cycle of that function.

```
//E7BJKPG1 JOB (E70021188B,T,E00053,003002),129,MSGLEVEL=1  P-GAIN
// EXEC FORTRANH
//SOURCE.SYSIN DD *
C  THIS PROGRAM HAS THE CAPABILITY TO CALCULATE AND PLOT POWER GAIN CURVES
C FOR ANALYTICALLY EXPRESSABLE CIRCULARLY SYMMETRIC SOURCE FUNCTIONS INCIDENT
C ON OBSTRUCTED AND UNOBSTRUCTED CIRCULAR APERTURES.  THE CURVES ARE RELATIVE
C TO A GAIN FACTOR (4*PI*A/WAVELENGTH**2), WHERE A IS THE APERTURE AREA.
C  THE OBSTRUCTIONS ARE ASSUME CIRCULAR AND CENTRALLY LOCATED WITHIN THE
C APERTURE.  THE INCIDENT FIELD IS ASSUMED NORMAL TO THE APERTURE WITH THE
C CAPABILITY OF BEING SEPARATED INTO AMPLITUDE AND PHASE COMPONENTS.
C  P-GAIN WAS WRITTEN SPECIFICALLY FOR LASER COMMUNCIATIONS FOR THE ANALYSIS
C OF CASSEGRAINIAN ANTENNAS.  TO OBTAIN THE REQUIRED ACCURACY IT WAS WRITTEN
C IN DOUBLE PRECISION.
C  ALL CALCULATIONS WERE MADE IN SPHERICAL COORDINATES AS DISPLAYED IN
C X-DOCUMENT X-524-73-185.
C
C PROGRAM P-GAIN - BEGIN MAIN
C
      IMPLICIT REAL*8 (B-H,O-Z)
C  THE LETTER A WILL NOT BE DEFINED TO BE DOUBLE PRECISION BUT USED FOR SINGLE
C PRECISION ARRAY NAMES BECAUSE WOLFPLOT PLOTTING ROUTINES WILL NOT ACCEPT
C DOUBLE PRECISION ARRAYS.
C  DEFINE AS COMPLEX THE FOLLOWING -
      COMPLEX*16 SUMEXP,FEXP,SEXP,DCONJG
C  FEXP - A FUNCTION EXTERNAL TO THE MAIN PROGRAM AND INTEGRAND OF THE COMPLEX
C INTEGRATION SUBROUTINE CDOG12
C  SEXP - THE RESULTANT OF THE COMPLEX INTEGRATION SUBROUTINE.
C  SUMEXP - THE SUM OF THE RESULTANTS FROM THE COMPLEX INTEGRATION SUBROUTINE.
C  DCONJG - A DOUBLE PRECISION EXTERNAL FUNCTION CONJUGATING SUMEXP.
C  DIMENSION AND DEFINE AS SINGLE PRECISION THE ARRAY NAMES;
      REAL*4 AGAIN(201),AGAIND(201),AX1(201)
C  AX1 = A PLOTTING PARAMETER FOR OFF AXIS DISTANCE WHICH ACCOUNTS FOR THE
C BEAM SPREAD.
C  AGAIN = GAIN
C  AGAIND = GAIN IN DECIBELS
C  DEFINE AS SINGLE PRECISION THE THREE VARIABLES YMIN, YSAVE, AND XSAVE WHICH
C SERVE AS VALUE HOLDERS DURING THE PLOTTING ROUTINE.
      REAL*4 YMIN,YSAVE,XSAVE
      DIMENSION NOCHAR(2)
      LOGICAL*1 BCHAR(8)
      DATA NOCHAR/+4,0/
      EXTERNAL FEXP,DCONJG
      COMMON DELTA,BETA,X1,GAMMA
C INITIALIZE THE WOLFPLOT PLOTTING ROUTINE
      CALL PLOTST (2001,4)
```

```
   10 FORMAT (3D15.5)
   20 FORMAT ('0',6X,'DELTA',11X,'BETA2',10X,'X1MAX',10X,'GAMMA')
   30 FORMAT (' THE PROGRAM HAS BEEN COMPLETED')
   40 FORMAT ('0',1X,'OFF AXIS DISTANCE',8X,'GAIN',14X,'GAIN IN DB')
   50 FORMAT (F13.4,6X,F13.4,9X,F13.4)
   60 FORMAT (2I2,D16.5)
   70 FORMAT (4D15.5)
      MTEST=0
C     MTEST IS USED AS A TEST FOR THE NUMBER OF DATA SETS (MCARDS) READ
   80 READ (5,60) NCARDS,MCARDS,X1MAX
C  MCARDS = THE NUMBER OF SETS OF DATA CARDS DICTATING THE NUMBER OF GRAPHS.
C  NCARDS = THE NUMBER OF CARDS IN A SET OF DATA CARDS DICTATING THE NUMBER OF
C CURVES PER GRAPH.
C  X1MAX = K*A*SIN(THETAMAX) WHERE A IS NOW THE APERTURE RADIUS, K IS THE
C PROPAGATION CONSTANT,THETAMAX IS A MAXIMUM ANGLE WHICH ACCOUNTS FOR THE
C PATTERN SPREAD, AND X1MAX IS CHOSEN AS THE MAXIMUM DISTANCE FROM THE AXIS
C THAT ONE WISHES TO OBSERVE THE PATTERN AND IS THE MAGNITUDE OF THE MAXIMUM
C VALUE OF THE ABSCISSA.
      AX1MAX=X1MAX
      AX1MIN=-X1MAX
C  AX1MAX AND AX1MIN ARE MAXIMUM AND MINIMUM X-AXIS PLOTTING PARAMETERS.
      MTEST=0
C  MTEST IS USED AS A TEST FOR A SET OF DATA CARDS (NCARDS) TO BE READ IN
C  INDIVIDUALLY.  EACH DATA CARD CONTAINS VALUES FOR DELTA, BETA, AND GAMMA.
      MTEST=MTEST+1
      CALL CONDNS
C  SET UP SUBJECT SPACE FOR PLOTTING
      CALL OGRID (AX1MIN,AX1MAX,10,'F5.1 ',1,-40.0,0.0,8,'F5.1 ',1,0)
C  COMPLETE TICK MARKS ALONG THE TOP BORDER OF THE GRAPH
      CALL OGRID (AX1MIN,AX1MAX,10,'F5.1 ',0,0.0,-40.0,0,'F5.1 ',0,10)
C  COMPLETE TICK MARKS ALONG THE RIGHT BORDER OF THE GRAPH
      CALL OGRID (AX1MAX,AX1MIN,0,'F5.1 ',0,-40.0,0.0,8,'F5.1 ',0,10)
   90 READ (5,10) DELTA,BETA2,GAMMA
C  DELTA = A/W0, WHERE A = APERTURE RADIUS AND W0 = THE GAUSSIAN BEAM WIDTH.
C  BETA2 = BETA/2PI
C  BETA = (K*A**2/2)*(1/R1+1/R), WHERE K=2*PI/WAVELENGTH, R=THE DISTANCE
C BETWEEN A POINT IN THE APERTURE AND THE OBSERVATION POINT, AND R1 IS THE
C DISTANCE FROM THE SOURCE TO THE POINT IN THE APERTURE.
C  GAMMA = B/A - THE FRACTION OF THE APERTURE TO BE OBSCURED, WHERE B = THE
C RADIUS OF THE CENTRAL OBSCURATION.
      NTEST=NTEST+1
      WRITE (6,20)
      WRITE (6,70) DELTA,BETA2,X1MAX,GAMMA
      WRITE (6,40)
      DO 170 I=1,101
```

```
      FSUB=I-1
C  DEFINE THE X-AXIS ARRAY AX1
      X1=X1MAX-FSUB*X1MAX/100.D0
      AX1(I)=X1
      K=202-I
      AX1(K)=-X1
      PI=3.1415926D0
      BETA=BETA2*2*PI
C  CALCULATE THE INTEGRAL NUMBER OF HALF CYCLES IN THE INTERVAL (0,1) BY (1)
C DIVIDING THE ARGUMENT OF THE COMPLEX EXPONENTIAL BY PI, WHICH IS N1, OR (2)
C DIVIDING THE ARGUMENT OF THE BESSEL FUNCTION BY PI, WHICH IS N2.
      N1=BETA/PI+1.D0
      N2=X1/PI+1.D0
C  WHICH OSCILLATES FASTER (THE EXPONENTIAL OR THE BESSEL FUNCTION) WILL
C DETERMINE THE NUMBER OF CYCLES OVER WHICH TO CARRY OUT THE INTEGRATION TO
C ASSURE ACCURACY OF THE SECONDARY PATTERN.  FARTHER FROM THE AXIS THE BESSEL
C FUNCTION IS ANTICIPATED TO OSCILLATE FASTER AND WILL THEREFORE RESULT IN A
C LARGER NUMBER OF HALF CYCLES TAKEN WITHIN THE ANNULUS OF THE APERTURE.
      NHCYC=MAXO(N1,N2)
C  INITIALIZE THE LOWER AND UPPER INTEGRATION LIMITS RL AND RH, RESPECTIVELY.
      RL=GAMMA**2
      IF (NHCYC.EQ.N1) GO TO 100
C  IF X1 EQUALS ZERO (THOUGH NOT LIKELY) AN ERROR WILL BE DETECTED IN COMPUTING
C RH IN THE NEXT STEP, THEREFORE TO AVOID THIS A TEST IS MADE FIRST.
      IF (X1.EQ.0.D0) GO TO 110
      RH=(PI/X1)**2
      GO TO 120
C  IF BETA EQUALS ZERO AN ERROR WILL BE DETECTED IN COMPUTING RH IN THE NEXT
C STEP, THEREFORE TO AVOID THIS A TEST IS MADE FIRST.
  100 IF (BETA.EQ.0.D0) GO TO 110
      RH=PI/BETA
      GO TO 120
  110 RH=1.D0
  120 CONTINUE
C  INITIALIZE INTEGRAL VALUES TO ZERO
      SUMEXP=(0.D0,0.D0
C  COMPUTE THE INTEGRALS
C  THE INTEGRATION IS CARRIED OUT OVER EACH HALF CYCLE AND SUMMED TOGETHER
C IN SUMEXP IN THE FOLLOWING DO LOOP.
      DO 150 J=1,NHCYC
C  TEST TO SEE IF LOWER LIMIT IS GREATER THAN UPPER LIMIT.  IF IT IS, THE
C PROGRAM JUMPS OVER A NUMBER OF STEPS TO READJUST RH.
      IF (RH.LE.RL) GO TO 130
      IF (RH.GT.1.D0) RH=1.D0
      CALL CDQG12 (RL,RH,FEXP,SEXP)
```

```
      SUMEXP=SUMEXP+SEXP
C  SET LOWER LIMIT EQUAL TO THE UPPER LIMIT AND ADD ONE MORE HALF CYCLE TO RH.
      RL=RH
  130 IF (NHCYC.EQ.N1) GO TO 140
C  LABLED LINE 23 TESTS FOR THE METHOD BY WHICH NHCYC WAS CHOSEN (N1,N2) SO
C AS TO DIRECT THE PROGRAM TO INCREMENT BY ONE HALF CYCLE THE CORRECT UPPER
C LIMIT RH.
      IF (X1.EQ.0.D0) GO TO 160
      RH=(DSQRT(RH)+PI/X1)**2
      GO TO 150
  140 IF (BETA.EQ.0.D0) GO TO 160
      RH=RH+PI/BETA
  150 CONTINUE
C  LABLED LINE 21 SERVES AS A JUMPING POINT OUTSIDE THE ABOVE LOOP TO AVOID
C REDUNDANT CALCULATIONS WHEN RL=RH.
  160 CONTINUE
C  COMPUTE THE VALUE OF THE GAIN
      BGAIN=2.D0*(DELTA**2)*SUMEXP*DCONJG(SUMEXP)
      AGAIN(I)=BGAIN
      AGAIN(K)=BGAIN
  170 CONTINUE
C  CONVERT THE GAIN DISTRIBUTION TO DECIBELS AND DEFINE THE Y-AXIS ARRAY AGAIND
      DO 180 I=1,201
      AGAIND(I)=10.*ALOG10(AGAIN(I))
  180 WRITE (6,50) AX1(I),AGAIN(I),AGAIND(I)
C  THE PROGRAM FROM THIS POINT TO LABEL 17 PLOTS THE GAIN DISTRIBUTION IN DB
C AND EXTRAPOLATES THE CURVE TO YMIN WHEN AGAIND FALLS BELOW YMIN.
      YMIN=-40.0
      I=1
      IF (AGAIND(1).LT.YMIN) GO TO 210
C  PLOT GAIN DISTRIBUTION ABOVE YMIN
  190 IO=I
      CALL INCORE (BETA2,BCHAR,15,1,5,2,0)
      DO 200 I=I,200
      IF (AGAIND(I+1).GE.YMIN) GO TO 200
      XSAVE=AX1(I+1)
      YSAVE=AGAIND(I+1)
      AX1(I+1)=AX1(I)+(AX1(I+1)-AX1(I))*(YMIN-AGAIND(I))/(AGAIND(I+1)-AG
     1AIND(I))
      AGAIND(I+1)=YMIN
      AHOLD=75.-IO
      CALL PLOTS (AX1(IO),AGAIND(IO),I+2-IO,0.0,0,0.0,0,0.0,0,1,0.0,0.0,
     10.0,0,BCHAR(2),NOCHAR,AHOLD,0,0)
      I=I+1
      AX1(I)=XSAVE
```

```
      AGAIND(I)=YSAVE
      GO TO 210
  200 CONTINUE
C  THIS PLOTS THE TAIL OF THE GAIN DISTRIBUTION ABOVE YMIN OR THE WHOLE
C DISTRIBUTION IF AGAIND NEVER DROPS BELOW YMIN.
      AHOLD=70.-10
      CALL PLOTS (AX1(10),AGAIND(10),202-10,0.0,0,0.0,0,0.0,0,1,0.0,0.0,
     10.0,0,BCHAR(2),NOCHAR,AHOLD,0,0)
      GO TO 230
  210 DO 220 I=1,200
      IF (AGAIND(I+1).LT.YMIN) GO TO 220
      AX1(I)=AX1(I)+(AX1(I+1)-AX1(I))*(YMIN-AGAIND(I))/(AGAIND(I+1)-AGAI
     1ND(I))
      AGAIND(I)=YMIN
      GO TO 190
  220 CONTINUE
C RETURN FOR NEW DATA CARD
  230 IF (NTEST.LT.NCARDS) GO TO 90
C  THE NEXT FOUR CALL STATEMENTS ARE TO LABEL THE AXES AND ADVANCE THE FRAME
C TO PLOT A NEW SET OF CURVES.
      CALL ROTLET (1.5708)
      CALL VERLIN ('BDC ROTCAF NIAG REWOP',22,.25,5.5,0,0)
      CALL ROTLET (0.0)
      CALL HORLIN ('X - K*A*SIN(THETA)',19,5.25,.60,0,0)
      CALL FRMADV
C RETURN FOR NEW DATA SET
      IF (MTEST.LT.MCARDS) GO TO 80
      CALL SETBLK (999)
      CALL ENDPLT
      WRITE (6,30)
      RETURN
      END
C  COMPLEX DOUBLE PRECISION GAUSSIAN INTEGRATION SUBROUTINE.
      SUBROUTINE CDQG12 (XL,XU,FCT,Y)
      IMPLICIT REAL*8 (A-H,O-Z)
      COMPLEX*16 FCT,Y
      A=.500*(XU+XL)
      B=XU-XL
      C=.49078031712335963D0*B
      Y=.23587668193255914D-1*(FCT(A+C)+FCT(A-C))
      C=.45205862818523743D0*B
      Y=Y+.53469662997659215D-1*(FCT(A+C)+FCT(A-C))
      C=.38495133709715234D0*B
      Y=Y+.80039164271673110-1*(FCT(A+C)+FCT(A-C))
      C=.29365897714330872D0*B
```

```
      Y=Y+.10158371336153296D0*(FCT(A+C)+FCT(A-C))
      C=.18391574949909010D0*B
      Y=Y+.11674626826917740D0*(FCT(A+C)+FCT(A-C))
      C=.62616704255734458D-1*B
      Y=B*(Y+.12457352290670139D0*(FCT(A+C)+FCT(A-C)))
      RETURN
      END
C  DOUBLE PRECISION BESSEL FUNCTION SUBROUTINE.
      SUBROUTINE DBESJ (X,N,BJ,D,IER)
      IMPLICIT REAL*8 (A-H,O-Z)
      BJ=0.D0
      IF (N) 10,20,20
   10 IER=1
      RETURN
   20 IF (X) 30,30,40
   30 IER=2
      RETURN
   40 IF (X-15.D0) 50,50,60
   50 NTEST=20.D0+10.D0*X-X**(2./3.)
      GO TO 70
   60 NTEST=90.D0+X/2.D0
   70 IF (N-NTEST) 90,80,80
   80 IER=4
      RETURN
   90 IER=0
      N1=N+1
      BPREV=0.D0
C
C     COMPUTE STARTING VALUE OF M
C
      IF (X-5.D0) 100,110,110
  100 MA=X+6.D0
      GO TO 120
  110 MA=1.4D0*X+60.D0/X
  120 IX=X
      MB=N+IX/4+2
      MZERO=MAXO(MA,MB)
C
C     SET UPPER LIMIT OF M
C
      MMAX=NTEST
      DO 210 M=MZERO,MMAX,3
C
C     SET F(M),F(M-1)
C
```

```
      FM1=1.0D-28
      FM=0.D0
      ALPHA=0.D0
      IF (M-(M/2)*2) 140,130,140
  130 JT=-1
      GO TO 150
  140 JT=1
  150 M2=M-2
      DO 180 K=1,M2
      MK=M-K
      BMK=2.D0*MK*FM1/X-FM
      FM=FM1
      FM1=BMK
      IF (MK-N-1) 170,160,170
  160 BJ=BMK
  170 JT=-JT
      S=1+JT
  180 ALPHA=ALPHA+BMK*S
      BMK=2.D0*FM1/X-FM
      IF (M) 200,190,200
  190 BJ=BMK
  200 ALPHA=ALPHA+BMK
      BJ=BJ/ALPHA
      IF (DABS(BJ-BPREV)-DABS(D*BJ)) 220,220,210
  210 BPREV=BJ
      IER=3
  220 RETURN
      END
C  DOUBLE PRECISION FUNCTION CONJUGATING THE COMPLEX INTEGRATION RESULTANT
C SEXP.
      COMPLEX FUNCTION DCONJG*16 (ARG)
      COMPLEX*16 ARG
      REAL*8 X,Y
      X=ARG
      Y=(0.D0,1.D0)*ARG
      DCONJG=X*(1.D0,0.D0)+Y*(0.D0,1.D0)
      RETURN
      END
C  DEFINE THE COMPLEX FUNCTION FEXP - THE INTEGRAND OF CDOG12.
      COMPLEX FUNCTION FEXP*16 (U)
      IMPLICIT REAL*8 (A-H,O-Z)
      COMPLEX*16 ARG
      COMMON DELTA,BETA,X1,GAMMA
   10 FORMAT (10X,I2)
      X=X1*DSQRT(U)
```

```
      EPS=1.D-05
      IF (X-EPS) 20,20,30
   20 BJ=1.0D0
      GO TO 50
   30 CALL DBESJ (X,0,BJ,EPS,IER)
      IF (IER.NE.0) GO TO 40
      GO TO 50
   40 WRITE (6,10) IER
C  AMP = THE AMPLITUDE OF THE INCIDENT SOURCE FUNCTION.
   50 AMP=DEXP(-(DELTA**2)*U)
C  DEFINE THE ARGUMENT OF THE EXPONENTIAL AS COMPLEX.
      ARG=(0.D0,1.D0)*BETA*U
      FEXP=CDEXP(ARG)*AMP*BJ
      RETURN
      END
/*
// EXEC LOADER,REGION.GO=200K
//GO.SYSLIB DD DSN=SYS2.WOLFPLOT,DISP=SHR
//GO.PLOTAPE  DD DCB=(,DEN=1),LABEL=(,BLP,,OUT),UNIT=(7TRACK,,DEFER),
//  DSN=BJKKLEIN,VOL=SER=(TD5600)
//GO.DATA5 DD *
 410          20.D00
       1.121D00          1.04D00          0.0D00
       1.121D00           1.4D00          0.0D00
       1.121D00          2.02D00          0.0D00
       1.121D00          2.44D00          0.0D00
 410          20.D00
       1.121D00           0.0D00          0.0D00
       1.121D00          0.52D00          0.0D00
       1.121D00          1.22D00          0.0D00
       1.121D00          1.71D00          0.0D00
 410          20.D00
       1.109D00          1.05D00          0.1D00
       1.109D00          1.41D00          0.1D00
       1.109D00          2.04D00          0.1D00
       1.109D00          2.47D00          0.1D00
 410          20.D00
       1.109D00           0.0D00          0.1D00
       1.109D00          0.53D00          0.1D00
       1.109D00          1.23D00          0.1D00
       1.109D00          1.73D00          0.1D00
 410          20.D00
       1.074D00          1.08D00          0.2D00
       1.074D00          1.46D00          0.2D00
       1.074D00           2.1D00          0.2D00
```

```
      1.074D00          2.55D00          0.2D00
410         20.D00
      1.074D00           0.0D00          0.2D00
      1.074D00          0.54D00          0.2D00
      1.074D00          1.27D00          0.2D00
      1.074D00          1.76D00          0.2D00
410         20.D00
      1.028D00          1.13D00          0.3D00
      1.028D00          1.55D00          0.3D00
      1.028D00          2.21D00          0.3D00
      1.028D00          2.69D00          0.3D00
410         20.D00
      1.028D00           0.0D00          0.3D00
      1.028D00          0.57D00          0.3D00
      1.028D00          1.34D00          0.3D00
      1.028D00          1.88D00          0.3D00
410         20.D00
      0.976D00          1.21D00          0.4D00
      0.976D00          1.69D00          0.4D00
      0.976D00          2.39D00          0.4D00
      0.976D00          2.92D00          0.4D00
410         20.D00
      0.976D00          0.00D00          0.4D00
      0.976D00          0.61D00          0.4D00
      0.976D00          1.45D00          0.4D00
      0.976D00          2.04D00          0.4D00
/*
```